



**UNIVERSITATEA
BABEȘ-BOLYAI**



Faculty of Chemistry and Chemical Engineering

**Group 15 (P, Sb) hypercoordinate compounds.
Synthesis, structure and reactivity.**

Răzvan Ioan ȘUTEU

PhD Thesis

Scientific advisor

Prof. Dr. Anca Silvestru

Cluj-Napoca

2022

Review committee

Chair: Prof. Dr. Ion Grosu
Universitatea Babeş-Bolyai, Cluj-Napoca

Scientific advisor: Prof. Dr. Anca Silvestru
Universitatea Babeş-Bolyai, Cluj-Napoca

Reviewers: CSI Dr. Otilia Costişor
Institutul de Chimie Coriolan Drăgulescu
al Academiei Române, Timișoara

Prof. Dr. Vasile Pârvulescu
Universitatea din București

Conf. Dr. Monica Venter
Universitatea Babeş-Bolyai, Cluj-Napoca

Keywords: hypercoordination, triarylphosphanes, triarylphosphane chalcogenides, group 11 metal complexes, organoantimony(iii) compounds, catalytic activity, structural investigation.

Table of Contents

I. Introduction	1
II. Organophosphorus ligands and their metal complexes	3
II.1. Literature data	3
II.2. Original contributions	8
II.2.1. Triarylphosphanes with 2-(Et₂NCH₂)C₆H₄ groups	9
II.2.2. Triorganophosphane sulfides and selenides	12
II.2.3. Group 11 metal complexes	24
II.3. Conclusions	40
III. Organoantimony compounds	41
III.1. Literature data	41
III.2. Original contributions	53
III.2.1. Diorganoantimony compounds with 2-(Me₂NCH₂)C₆H₄ groups	53
III.2.2. Diorganoantimony compounds containing the C₆H₅CH₂N(CH₂C₆H₄)₂ fragment	63
III.2.3. Diorganoantimony compounds containing the C₆H₅CH₂CH₂N(CH₂C₆H₄)₂ fragment	73
III.2.4. Diorganoantimony compounds containing the CH₃OCH₂CH₂N(CH₂C₆H₄)₂ fragment	82
III.2.5. Hypercoordinated triorganoantimony(III) compounds with organic groups bearing two CH₂NMe₂ pendant arms	Error! Bookmark not defined.
III.3. Catalytic results and theoretical calculations	92
III.4. Conclusions	95
IV. Experimental section	97
IV.1. General experimental details	97
IV.2. Synthesis	98
Synthesis of [2-(Et ₂ NCH ₂)C ₆ H ₄]Br	98
Synthesis of [2-(Et ₂ NCH ₂)C ₆ H ₄]Li.....	98
Synthesis of (2-BrC ₆ H ₄ CH ₂) ₂ NCH ₂ C ₆ H ₅	99
Synthesis of (2-BrC ₆ H ₄ CH ₂) ₂ NCH ₂ CH ₂ C ₆ H ₅	99
Synthesis of (2-BrC ₆ H ₄ CH ₂) ₂ NCH ₂ CH ₂ OCH ₃	100
Synthesis of [2-(Et ₂ NCH ₂)C ₆ H ₄]Ph ₂ P (1)	100
Synthesis of [2-(Et ₂ NCH ₂)C ₆ H ₄] ₂ PhP (2)	101
Synthesis of [2-(Et ₂ NCH ₂)C ₆ H ₄]Ph ₂ PS (3)	101
Synthesis of [2-(Et ₂ NCH ₂)C ₆ H ₄]Ph ₂ PSe (4)	102
Synthesis of [2-(Et ₂ NCH ₂)C ₆ H ₄] ₂ PhPS (5)	102
Synthesis of [2-(Et ₂ NCH ₂)C ₆ H ₄] ₂ PhPSe (6)	103

Synthesis of [2-(Et ₂ NCH ₂)C ₆ H ₄]Ph ₂ PCuCl (7)	103
Synthesis of [2-(Et ₂ NCH ₂)C ₆ H ₄]Ph ₂ PAgOTf (8)	104
Synthesis of [2-(Et ₂ NCH ₂)C ₆ H ₄]Ph ₂ PAuCl (9)	104
Synthesis of [2-(Et ₂ NCH ₂)C ₆ H ₄] ₂ PhPCuCl (10)	105
Synthesis of [2-(Et ₂ NCH ₂)C ₆ H ₄] ₂ PhPAgOTf (11)	106
Synthesis of [2-(Et ₂ NCH ₂)C ₆ H ₄] ₂ PhPAuCl (12)	106
Synthesis of [2-(Me ₂ NCH ₂)C ₆ H ₄] ₂ SbCl (13).....	107
Synthesis of [2-(Me ₂ NCH ₂)C ₆ H ₄] ₂ SbONO ₂ (14)	107
Synthesis of [2-(Me ₂ NCH ₂)C ₆ H ₄] ₂ SbOSO ₂ CF ₃ (15)	108
Synthesis of [C ₆ H ₅ CH ₂ N(CH ₂ C ₆ H ₄) ₂]SbCl (16).....	108
Synthesis of [C ₆ H ₅ CH ₂ N(CH ₂ C ₆ H ₄) ₂]SbONO ₂ (17).....	109
Synthesis of [C ₆ H ₅ CH ₂ N(CH ₂ C ₆ H ₄) ₂]SbOSO ₂ CF ₃ (18).....	109
Synthesis of [C ₆ H ₅ CH ₂ CH ₂ N(CH ₂ C ₆ H ₄) ₂]SbCl (19).....	110
Synthesis of [C ₆ H ₅ CH ₂ CH ₂ N(CH ₂ C ₆ H ₄) ₂]SbONO ₂ (20)	110
Synthesis of [C ₆ H ₅ CH ₂ CH ₂ N(CH ₂ C ₆ H ₄) ₂]SbOSO ₂ CF ₃ (21)	111
Synthesis of [CH ₃ OCH ₂ CH ₂ N(CH ₂ C ₆ H ₄) ₂]SbCl (22).....	112
Synthesis of [CH ₃ OCH ₂ CH ₂ N(CH ₂ C ₆ H ₄) ₂]SbONO ₂ (23)	112
Synthesis of [CH ₃ OCH ₂ CH ₂ N(CH ₂ C ₆ H ₄) ₂]SbOSO ₂ CF ₃ (24)	113
Synthesis of [2,6-(Me ₂ NCH ₂) ₂ C ₆ H ₃] ₂ PhSb (25).....	113
IV.3. Catalysis.....	114
References.....	115
Appendix.....	121
List of relevant publications.....	134
List of relevant conferences.....	134
Acknowledgements	135

I. Introduction

Ligands are of great importance in coordination chemistry because they can strongly influence the chemical and physical properties of the metal complexes. Usually, a rational combination of ligands and metal centers is used to design metal complexes with specific properties which recommend them as valuable candidates for various applications in biology, catalysis or materials science.^[1]

The donor ability, the number and the type of the donor atoms, the structure and the flexibility of the skeleton of a desired ligand are important factors which should be considered in order to predict further electronic and steric effects resulted by coordination to certain metals or organometallic fragments. The possibilities to control carefully the electronic environment around the metal center and, consequently, the reactivity and the stability of the designed metal complexes, are of continuously increased interest and a high number of papers describing new coordination compounds are published each year.

Transition metals, due to their specific properties and their disponibility to accommodate electron pairs from various ligands in their free orbitals, were largely used in coordination chemistry and their complexes found applications as catalysts (e.g. Pd, Pt, Rh, Ir, Ru compounds)^[2] or as antitumor or antibacterial agents (e.g. Pt, Ag, Au containing species).^[3] At a lesser extent were investigated main group metal and organometallic compounds, both in catalysis and in biology. It was observed that main group organometallic complexes can be stabilized by using either bulky organic groups or aromatic groups decorated with pendant arms and donor atoms, capable for intramolecular E→M interactions (E = N, O, S, Se), which can generate hypercoordinated species.^[4] According to Arduengo, hypervalent or hypercoordinated compounds are those based on main group elements surrounded by more than eight electrons in their coordination sphere and they can be designated as *N-X-L* species, where N = number of electrons about the metal X and L = number of donor atoms directly bond to the metal X.^[4b]

The presence of such bonds has attracted considerable interest, especially in last decades, since it strengthens the thermal and hydrolytic stability, influence the chemical reactivity, the biological properties and allows the access to novel types of compounds which are convenient models for studying fundamental applications. A large number of publications discuss their role in *(i)* stabilization of main group elements in their low oxidation states, *(ii)* design of chiral species with significant catalytic activity, *(iii)* single source precursors for MOCVD, *(iv)* active therapeutic agents, *(v)* formation of supramolecular networks.

The present work presents the original contributions brought by the studies performed on the chemistry of hypervalent organophosphorus(III) and organoantimony(III) compounds containing aromatic organic groups with potential for intramolecular N→E (E = P, Sb) interactions. Literature data relevant for the new compounds discussed in this work are also presented.

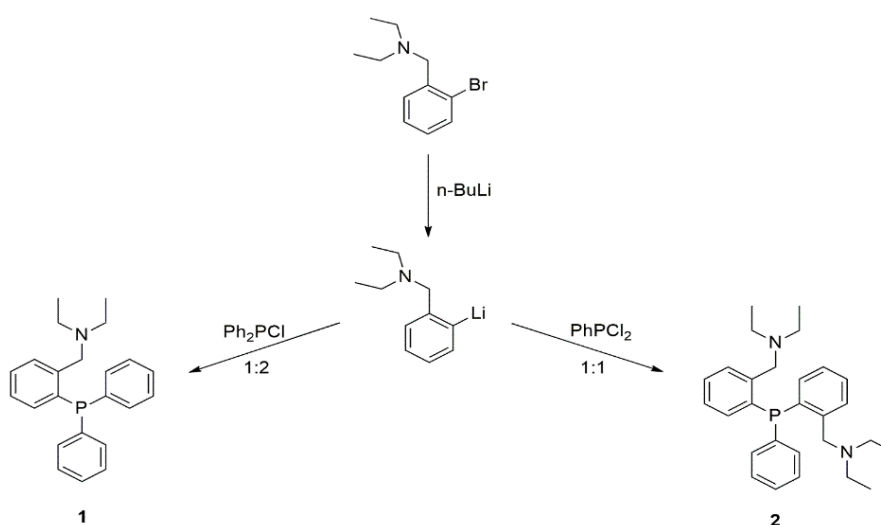
In this work are described triorganophosphanes of type $[2-(\text{Et}_2\text{NCH}_2)\text{C}_6\text{H}_4]_n\text{Ph}_{3-n}\text{P}$ ($n = 0-2$) and organoantimony complexes of types $[2-(\text{Me}_2\text{NCH}_2)\text{C}_6\text{H}_4]_2\text{SbX}$ ($X = \text{Cl}, \text{OTf}, \text{ONO}_2$) and $[\text{RN}(\text{CH}_2\text{C}_6\text{H}_4)_2]\text{SbL}$ ($\text{R} = \text{Bn}, \text{PhCH}_2\text{CH}_2, \text{MeOCH}_2\text{CH}_2, \text{L} = \text{Cl}, \text{OTf}, \text{ONO}_2$). The triorganophosphanes were employed as *P,N* ligands towards copper (I), silver(I) and gold(I) salts and were oxidized to the triorganophosphane chalcogenides $[2-(\text{Et}_2\text{NCH}_2)\text{C}_6\text{H}_4]_n\text{Ph}_{3-n}\text{PE}$ ($\text{E} = \text{S}, \text{Se}$), while the antimony(III) compounds were investigated as catalysts in the Henry (nitroaldol) reaction.

II. Organophosphorus ligands and their metal complexes.

II.2.1. Triarylphosphanes with 2-(Et₂NCH₂)C₆H₄ groups

Preparation

$[2-(\text{Et}_2\text{NCH}_2)\text{C}_6\text{H}_4]\text{Ph}_2\text{P}$ (**1**) and $[2-(\text{Et}_2\text{NCH}_2)\text{C}_6\text{H}_4]_2\text{PhP}$ (**2**) were prepared using a similar procedure as that one described in literature for compounds bearing 2-Me₂NCH₂ pendant arms, slightly modified due to the higher sensitivity to moisture and oxygen. Phosphanes **1** and **2** were isolated as colorless oils and stored in the glovebox, under inert atmosphere. The reactions employed in the synthesis are presented in Scheme II.1.



Scheme II.1.

NMR spectroscopy

The solution behavior of all these compounds was investigated by multinuclear NMR (^1H , ^{13}C , ^{31}P) spectroscopy. From the NMR spectra the presence of the expected organic moieties was confirmed in each case. The ^1H NMR spectra of phosphanes **1** and **2** are shown in Figures II.1 and II.2, respectively.

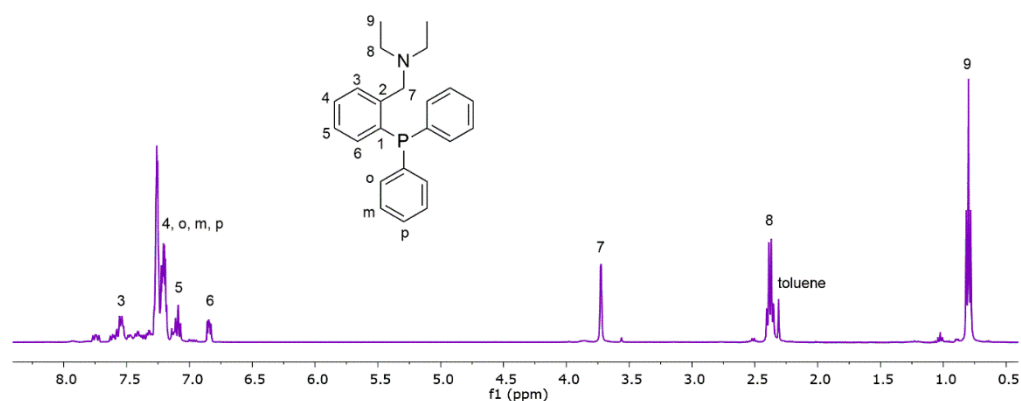


Figure II.1. ^1H NMR spectrum of compound **1**, in CDCl_3 .

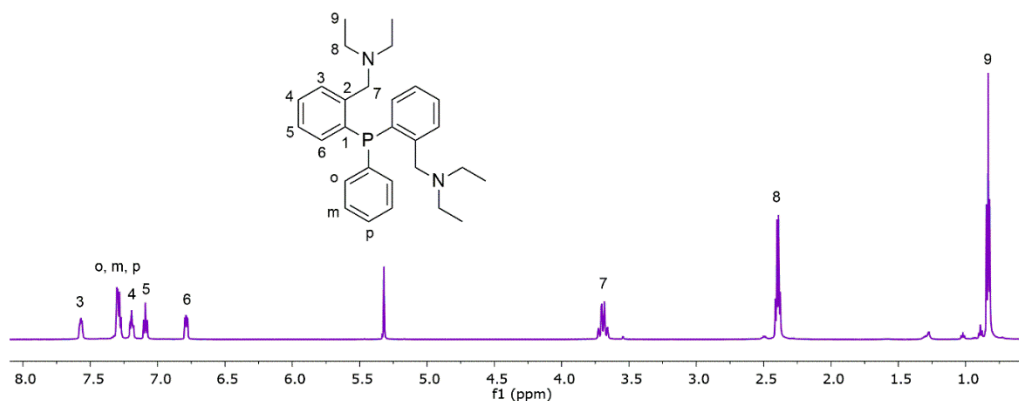


Figure II.2. ^1H NMR spectrum of compound **2**, in CD_2Cl_2 .

For compound **2**, bearing two 2-(Et_2NCH_2) C_6H_4 groups, the NMR spectrum suggests their equivalence in solution. The ^1H NMR resonances of the $\text{CH}_2\text{N}(\text{CH}_2\text{CH}_3)_2$ moieties bring no clear evidence for an intramolecular $\text{N}\rightarrow\text{P}$ coordination in solution, at least in case of compound **1**, for which a broad singlet was assigned for the CH_2N protons. By contrast, an ABX spin system was observed in the ^1H NMR spectrum of **2** for the nonequivalent CH_2N protons, thus suggesting the existence of an intramolecular $\text{N}\rightarrow\text{P}$ coordination in this case. The ^{31}P NMR spectra in Figure II.3 present in both cases only one singlet resonance, thus being consistent with the presence of only one species in solution.

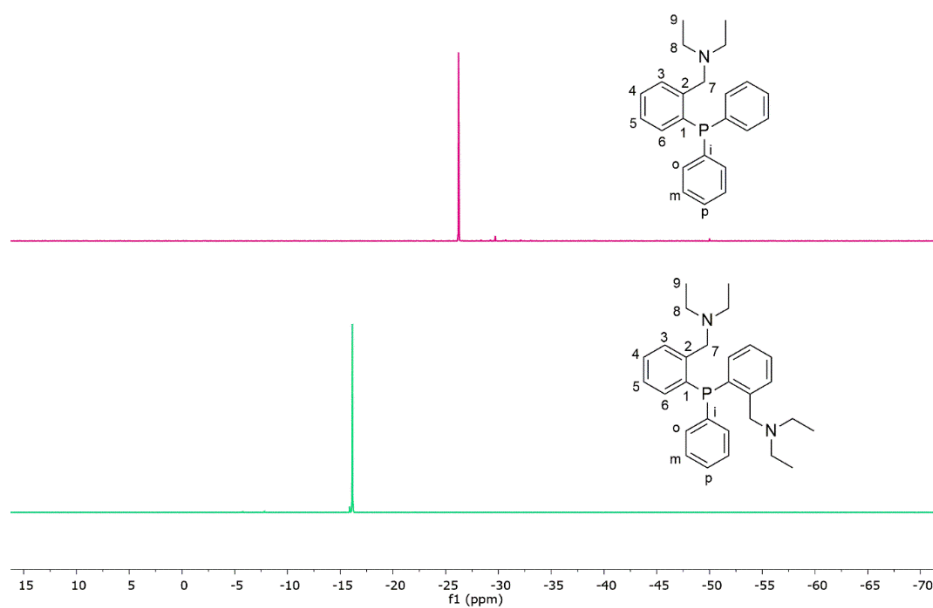
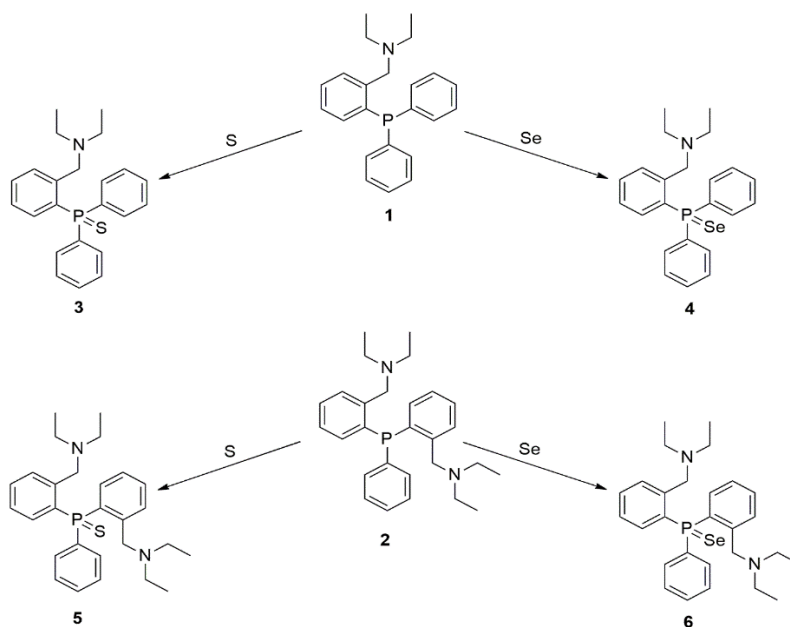


Figure II.3. ^{31}P NMR spectrum of compounds **1**(up) and **2**(down), in CDCl_3 .

II.2.2. Triorganophosphane sulfides and selenides

Preparation

Oxidation of the starting phosphanes **1** and **2** with elemental sulphur or selenium powder, under anhydrous conditions, was performed as depicted in Scheme II.2.



Scheme II.2.

The obtained phosphane chalcogenides **3-6** were isolated as pale-yellow microcrystalline solids, soluble in common organic solvents.

NMR spectroscopy

The NMR spectra (Figures 4 and 5) confirmed the expected composition and structure. For the triorganophosphane chalcogenides **3** and **4**, bearing one 2-(Et₂NCH₂)C₆H₄ group, only broad resonances were observed in the aliphatic region, while for compounds **5** and **6**, with two 2-(Et₂NCH₂)C₆H₄ groups, the resonances for the aliphatic protons are well resolved, giving rise to a triplet and a quartet for the ethyl protons and an AB spin system for the diastereotopic C₆H₄CH₂N protons.

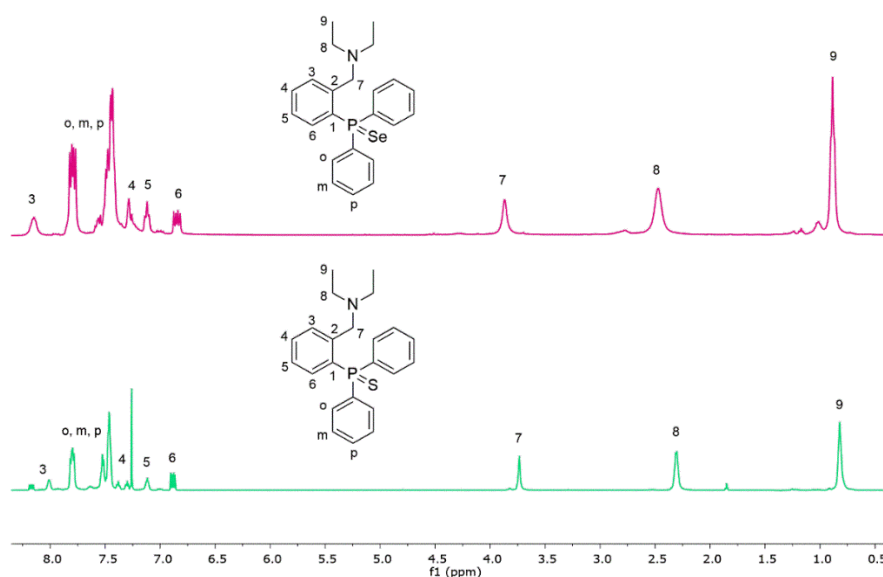


Figure II.4. ¹H NMR spectra of compounds **3** (down) and **4** (up), in CDCl₃.

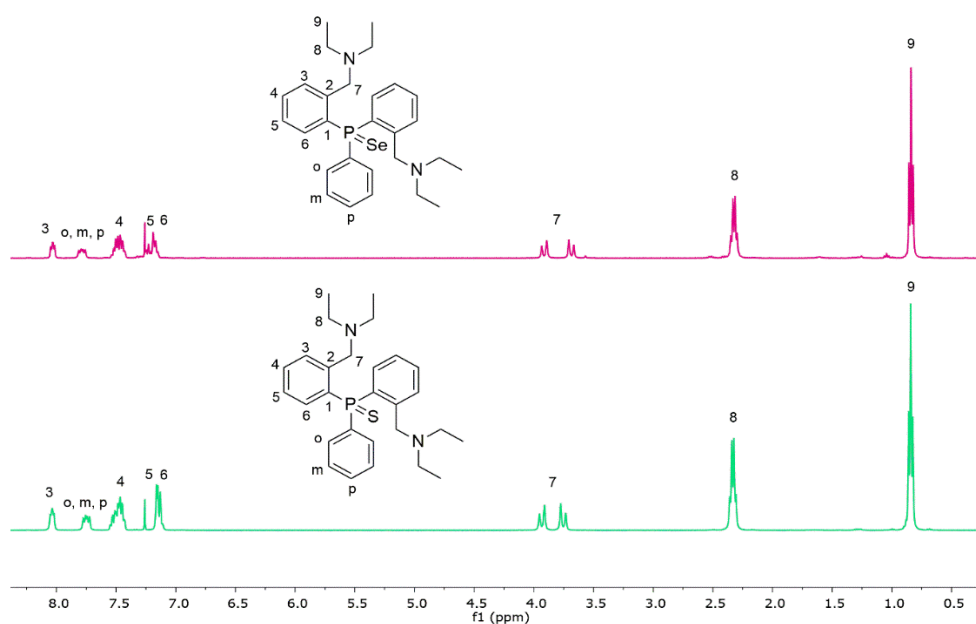


Figure II.5. ¹H NMR spectra of compounds **5** (down) and **6** (up), in CDCl₃.

The ^1H NMR spectra suggest a dynamic behavior in solution, at room temperature, for compounds **3** and **4**, involving decoordination, inversion at nitrogen and re-coordination, while for compounds **5** and **6** we assume that the intramolecular coordination is preserved in solution even at room temperature.

The ^{31}P NMR spectra present for each of these four compounds only one singlet resonance, thus being consistent with the presence of only one species in solution. In the case of compounds **4** and **6**, due to the direct bond between the phosphorus atom and the selenium atom, selenium satellites are observed in their ^{31}P NMR spectra, determined by ^{31}P - ^{77}Se NMR couplings.

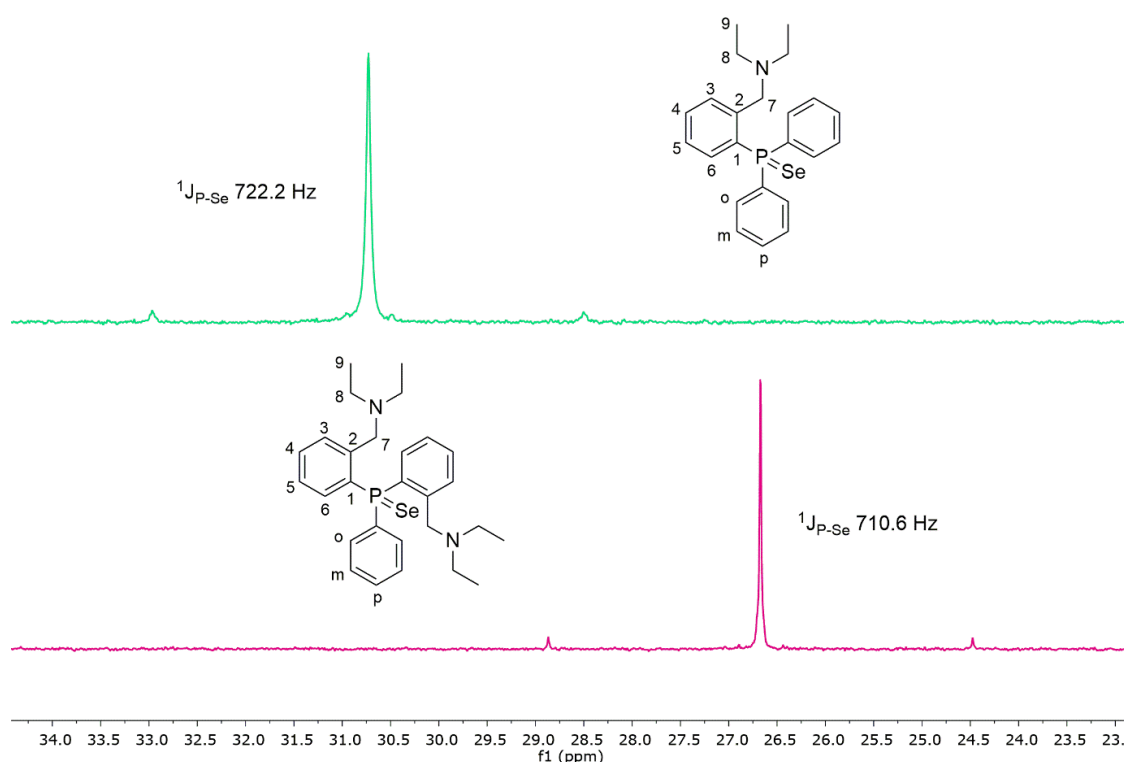


Figure II.6. ^{31}P NMR spectra of compounds **4** (up) and **6** (down), in CDCl_3 .

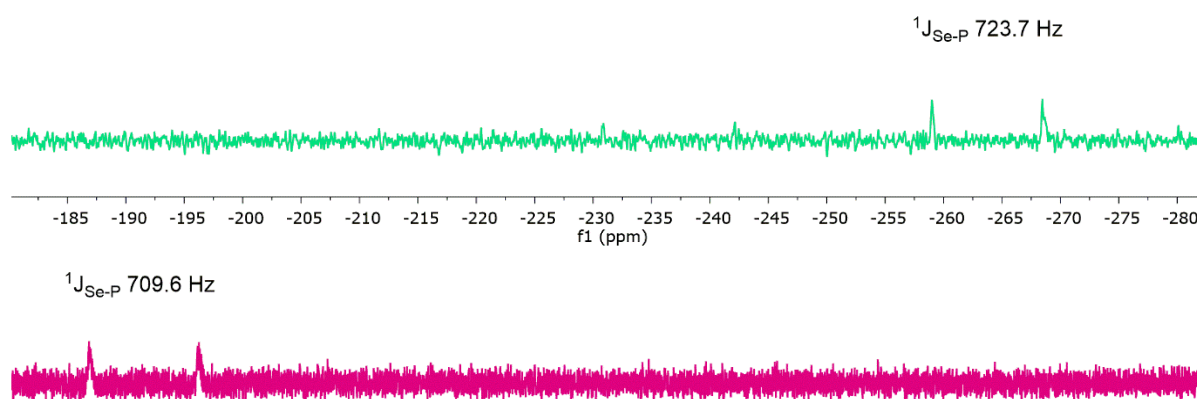


Figure II.7. ^{77}Se NMR spectra of compounds **4** (up) and **6** (down), in CDCl_3 .

Consequently, for compound **4** a doublet was observed in the ^{77}Se NMR at δ -263.1 ppm, with a coupling constant $^1J_{\text{Se-P}}$ of 723.7 Hz, almost identical to the value found in the ^{31}P NMR spectrum of this compound, $^1J_{\text{P-Se}}$ 722.2 Hz. Similarly, in the case of compound **6** the same interactions could be observed, a doublet in the ^{77}Se NMR at δ -191.5 ppm, with a coupling constant $^1J_{\text{Se-P}}$ of 709.6 Hz, almost identical to the value found in the ^{31}P NMR spectrum of this compound, respectively $^1J_{\text{P-Se}}$ 710.6 Hz (Figure II.7.)

Mass spectrometry

ESI+ MS studies were performed for the triarylphosphane chalcogenides. In every case the spectra present the peaks characteristic for the pseudo-molecular ion $[\text{M} + \text{H}^+]$ (top) and the simulated peak for the compound (bottom). The ESI+ mass spectrum of compound **4** presents the characteristic peak for the pseudo-molecular ion $[\{2-(\text{Et}_2\text{NCH}_2)\text{C}_6\text{H}_4\}\text{Ph}_2\text{PSe} + \text{H}^+]$ at m/z 428.1035 (Figure II.8).

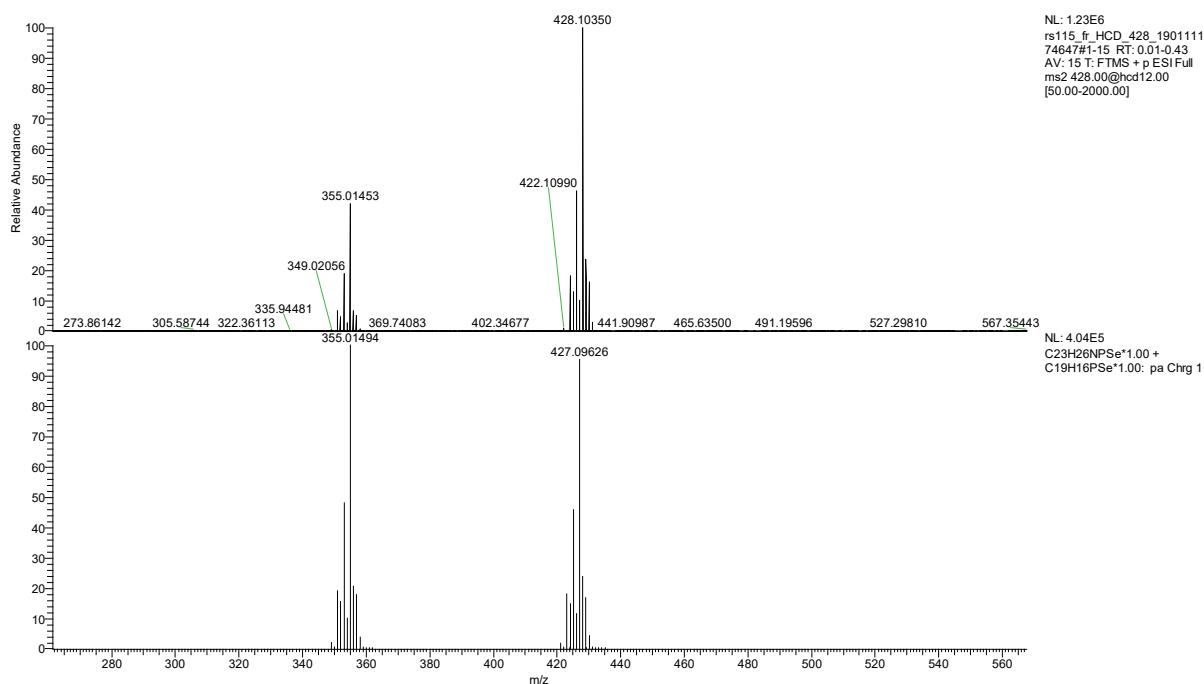


Figure II.8. ESI+ mass spectrum of compound **4** showing the peaks at m/z 355.0145 (43) $[\text{M} - \text{NEt}_2 + \text{H}^+]$ and at m/z 428.1035 (100) $[\text{M} + \text{H}^+]$.

Single-crystal X-ray diffraction studies

Single-crystals suitable for X-ray diffraction studies were obtained for the chalcogenides **3**, **4** and **5**, the molecular structures are depicted in Figures II.9, Figure II.10 and

Figure II.11, respectively. Compound **3** displays a monomeric structure, with a distorted tetrahedral coordination geometry around the phosphorus atom. In both compounds **3** and **4**, the P=S interatomic distance is consistent with a double bond (1.947(3) Å).

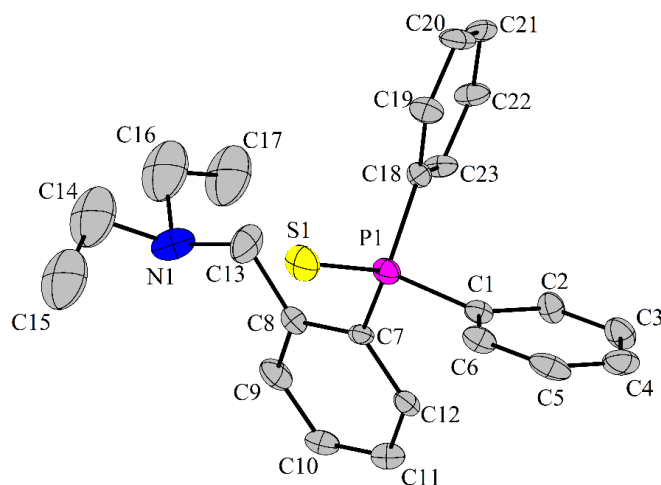


Figure II.9. Ortep-like representation of compound **3**, with thermal ellipsoids at 20% probability level. Hydrogen atoms were omitted for clarity.

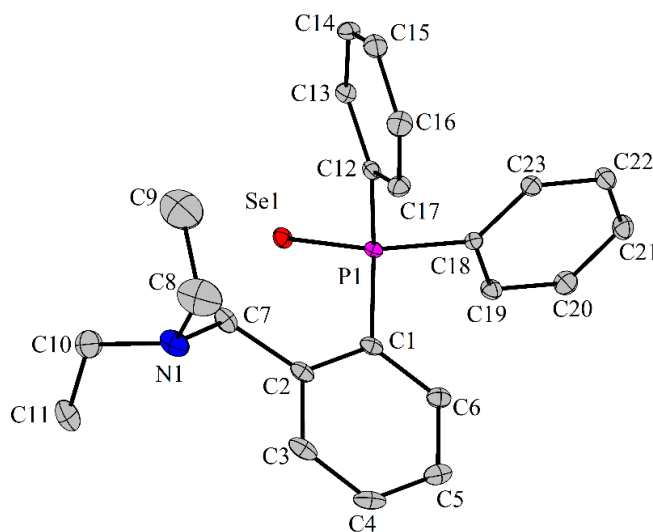


Figure II.10. Ortep-like representation of compound **4**, with thermal ellipsoids at 30% probability level. Hydrogen atoms were omitted for clarity.

In the case of compound **4** a distorted tetrahedral coordination geometry is realized around the phosphorus atom as well, with bond angles ranging from 106.6(1)° (C1–P1–C18) to 114.2(8)° (C12–P1–Se1). As expected, the P=Se interatomic distance is consistent with a double bond of 2.114(7) Å.

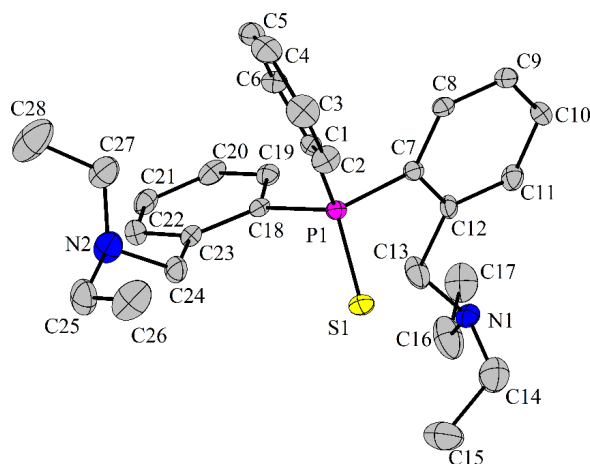


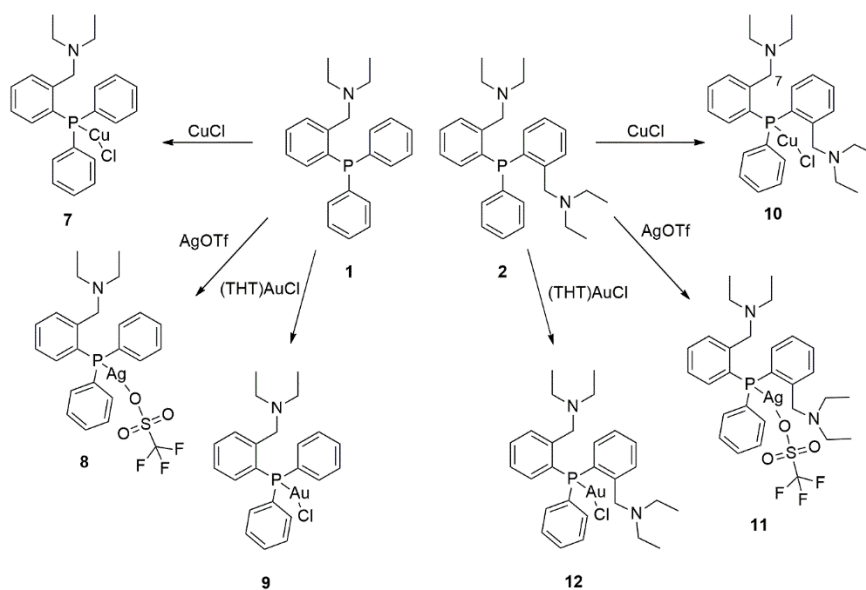
Figure II.11. Ortep-like representation of compound **5**, with thermal ellipsoids at 30% probability level. Hydrogen atoms were omitted for clarity.

Compound **5** displays a monomeric structure, with a distorted tetrahedral coordination geometry around the phosphorus atom, with bond angles varying from $103.45(19)^\circ$ (C1–P1–C18) to $116.60(14)^\circ$ (C18–P1–S1).

II.2.3. Group 11 metal complexes

Preparation

The metal complexes **7**, **9**, **10** and **12** were isolated as colorless solids, whereas the silver containing compounds **8** and **11** could not be isolated in a pure form, due to decomposition. The copper complexes **7** and **10** are stable at room temperature in the presence of air, while the gold complexes **9** and **12** are air stable only at low temperatures.



Scheme II.3.

NMR spectroscopy

All metal complexes were investigated in solution by multinuclear NMR (^1H , ^{13}C , ^{31}P). For the species containing triflate ligands, ^{19}F NMR was also employed for their characterization. The desired composition and purity were confirmed in each case.

For compounds 7 and 10 broad signals can be observed in the ^{31}P NMR, thus suggesting the direct bonding of the phosphorus to the metal center.

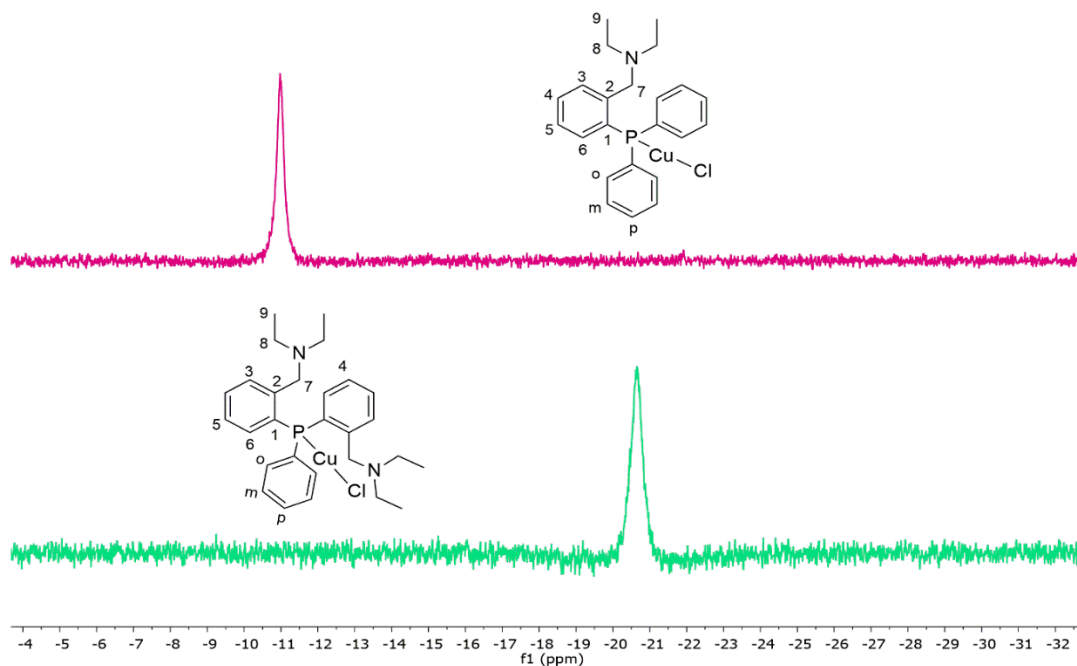


Figure II.12. ^{31}P NMR spectra of complexes 7 (up) and 10 (down), in CDCl_3 .

The silver complexes showed broad resonances, thus suggesting a dynamic behavior in solution and, possibly, the existence of minor species in equilibrium with the major compound.

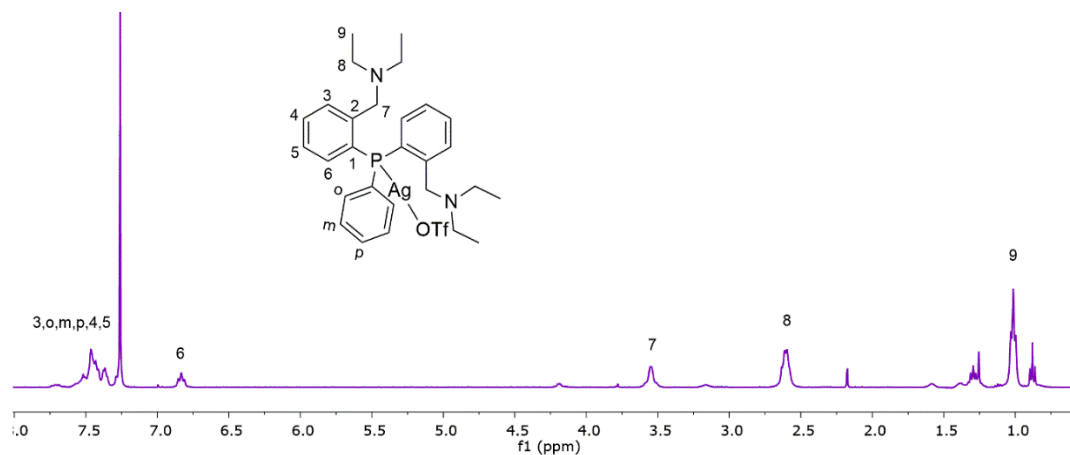


Figure II.13. ^1H NMR spectrum of complex **11**, in CDCl_3 .

The ^{19}F NMR spectra of the silver complexes (Figure II.14) display one sharp singlet in each case around -77 ppm. This confirms the presence of fluorine in the complex and the formation of the silver(I) complex.

While in the case of complex **8** a very broad singlet was observed, in the case of complex **11** the presence of a doublet with broad bands confirms the formation of a phosphorus-silver bond, with a characteristic coupling constant $^1J_{\text{P-Ag}} = 616.1$ Hz (Figure II.15).

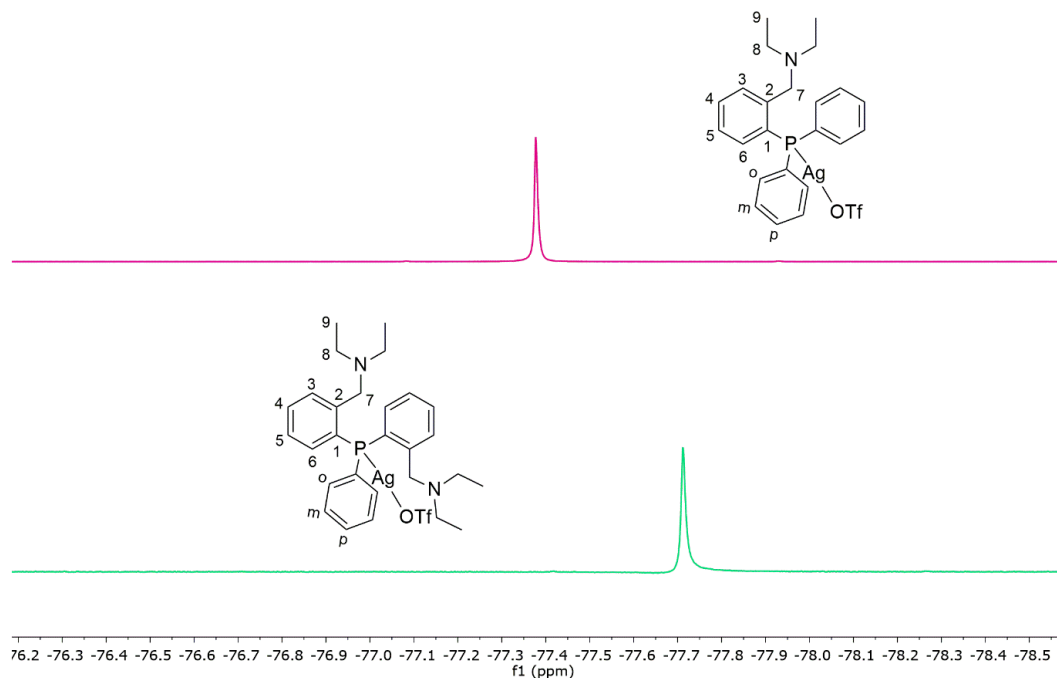


Figure II.14. ^{19}F NMR spectrum of complexes **8** (up) and **11** (down), in CDCl_3 .

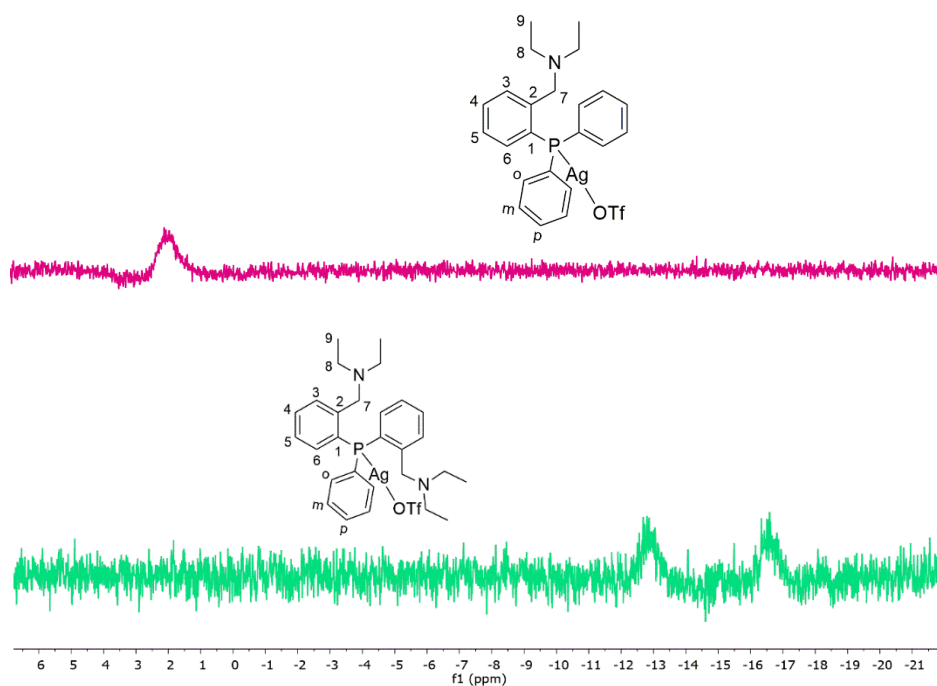


Figure II.15. ^{31}P NMR spectrum of complexes **8** (up) and **11** (down), in CDCl_3 .

In the case of the gold complexes the resonances corresponding to the ethyl protons in both compounds are resolved in a triplet and a quartet. Concerning the $\text{C}_6\text{H}_4\text{CH}_2\text{N}$ protons, they appear as a singlet, in complex **9**, thus suggesting a dynamic behavior of the pendant arm in solution. For complex **12**, the presence of an AB spin system suggests a different behavior for the $\text{C}_6\text{H}_4\text{CH}_2\text{N}$ protons, i.e. the free movement of the pendant arms is prevented.

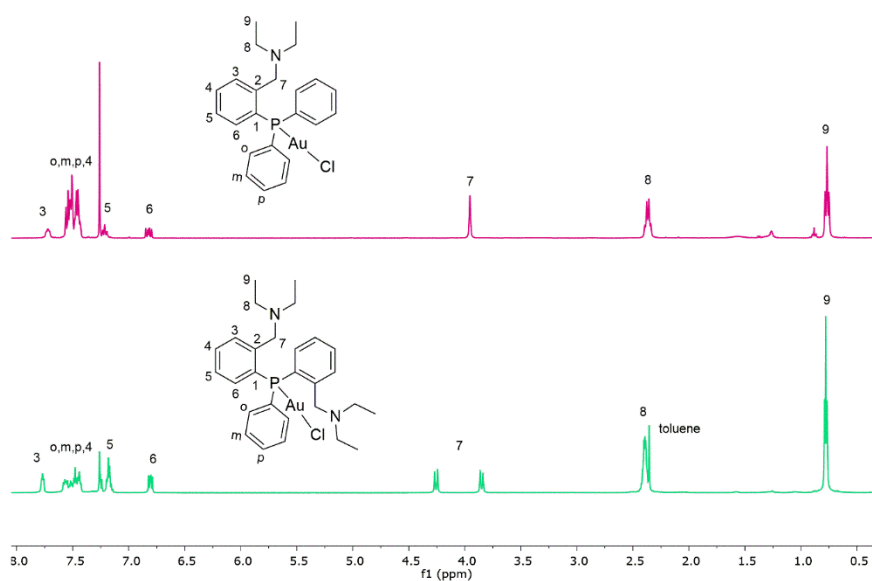


Figure II.16. ^1H NMR spectrum of complexes **9** (up) and **12** (down), in CDCl_3 .

In both cases the expected resonances can be observed in the ^{31}P NMR (Figure II.17).

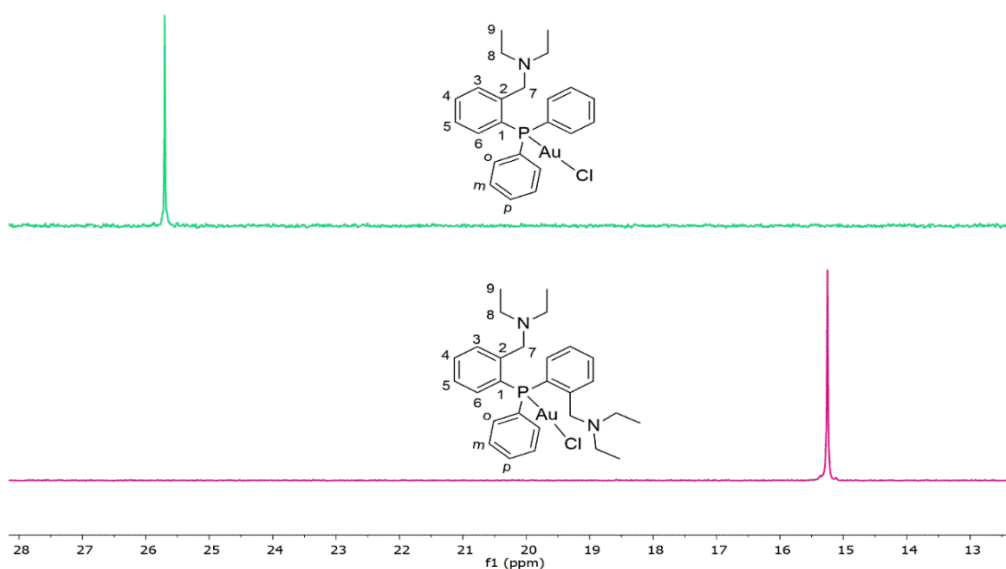


Figure II.17. ^{31}P NMR spectrum of complexes **9** (up) and **12** (down), in CDCl_3 .

Mass spectrometry

ESI+ MS studies were performed for all metal complexes. In some cases, the spectra present the peaks characteristic for the pseudo-molecular ion $[\text{M} + \text{H}^+]$, while for the others only the peaks characteristic for the cations formed by chlorine elimination, was observed. In case of complex **7**, the peak corresponding for the cation $[\{2-(\text{Et}_2\text{NCH}_2)\text{C}_6\text{H}_4\}\text{Ph}_2\text{PCu}]^+$ was observed as a base peak at $m/z = 410.1109$. In the case of complex **10**, the peak for the pseudo-molecular ion $[\{2-(\text{Et}_2\text{NCH}_2)\text{C}_6\text{H}_4\}_2\text{PhPCuCl} + \text{H}^+]$ was present at $m/z = 531.1768$ with a lower intensity, while the base peak is displayed at $m/z = 495.1999$ and corresponds to the cation $[\{2-(\text{Et}_2\text{NCH}_2)\text{C}_6\text{H}_4\}_2\text{PhPCu}]^+$.

Single-crystal X-ray diffraction studies

The copper complexes **7** and **10** formed dimeric associations, with a distorted tetrahedral geometry around each copper atom. The triorganophosphane ligand, in both compounds, acts as a bidentate chelating P,N moiety towards the copper center. The dimeric association is realized in both compounds by bridging chlorine atoms ($\text{Cu1}\cdots\text{Cl1}'$ 2.3593(9) Å in **7** and 2.3317(13) Å in **10**, vs. $\Sigma r_{\text{vdW}}(\text{Cu},\text{Cl})$ 3.20 Å ^[12]).

In complex **10** the two $2-(\text{Et}_2\text{NCH}_2)\text{C}_6\text{H}_4$ groups that are attached to the phosphorus atom behave in opposite ways, more precisely, one of them is intramolecularly coordinated to the copper centre through a strong $\text{N}\rightarrow\text{Cu}$ interaction (2.19 Å vs. $\Sigma r_{\text{vdW}}(\text{Cu},\text{N})$ 2.94 Å ^[12]), at

that time the other one remains hanging free, with the N2/N2' atoms forced far away from the coordination sphere of phosphorus or copper.

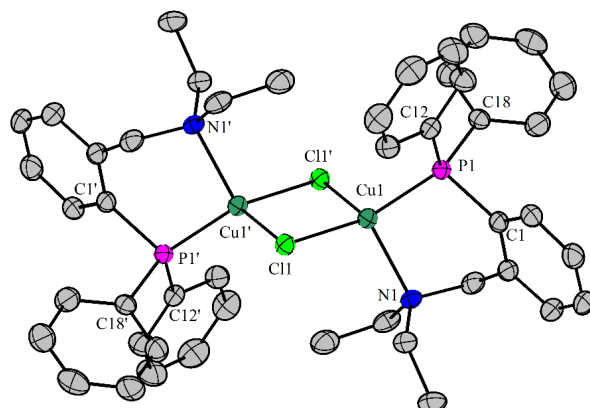


Figure II.18. Ortep-like representation of compound **7**, with thermal ellipsoids at 30% probability level. Hydrogen atoms were omitted for clarity.

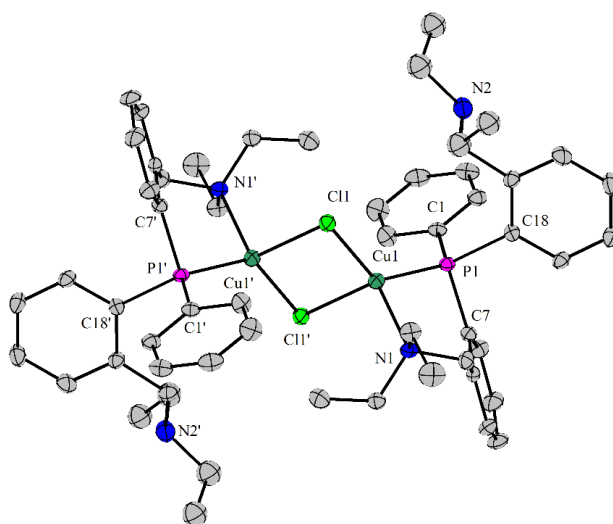


Figure II.19. Ortep-like representation of compound **10**, with thermal ellipsoids at 30% probability level. Hydrogen atoms were omitted for clarity.

The intramolecular N→Cu interaction gives rise to two six membered CuPC₃N rings in each case. These rings are not planar, they are folded around the imaginary axes P1⋯C7 and P1'⋯C7' in **7** and P1⋯C13 and P1'⋯C13' in **10**, presenting twisted boat conformations.

A planar chirality is induced by the intramolecular N→Cu coordination.^[47] The complexes crystallized as a mixture of *R* and *S* isomers that are interconnected in *R*_{N1}, *S*_{N1'} and *S*_{N1}, *R*_{N1'} dimers in both cases. By applying the skew line convention,^[47] the structure of the copper complexes might be discussed in terms of λ and δ isomers. Therefore, compounds **7** and **10** crystallize as a racemate of $\lambda_{\text{Cu1}}/\delta_{\text{Cu1'}}$ and $\delta_{\text{Cu1}}/\lambda_{\text{Cu1'}}$ dimers, where δ and λ refer to the chirality of the six-membered chelate rings associated with copper.

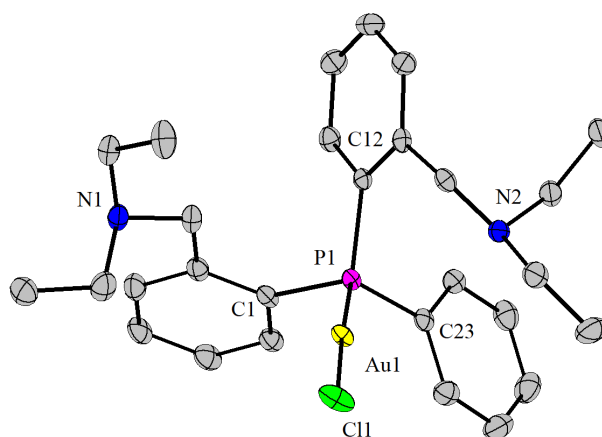


Figure II.20. Ortep-like representation of compound **12**, with thermal ellipsoids at 50% probability level. Hydrogen atoms were omitted for clarity.

The gold complex **12** has a monomeric structure, with a linear geometry around the gold center, the Cl1–Au1–P1 angle is almost linear ($176.78(2)^\circ$). In this case the triorganophosphane ligand does not behave as a chelating agent towards the metal center,

The molecules are associated into polymeric chains in which the chlorine atom from one molecule forms with one hydrogen atom from the phenyl ring of a neighboring molecule a hydrogen...halogen interaction (H24...Cl1 2.73 Å).

II.3. Conclusions

- Two new phosphanes, [2-(Et₂NCH₂)C₆H₄]Ph₂P (**1**) and [2-(Et₂NCH₂)C₆H₄]₂PhP (**2**), were obtained as yellowish oils and they were structurally characterized in solution.
- The phosphanes **1** and **2** were used in oxidation reactions with elemental chalcogens (sulphur and selenium), thus resulting four new triorganophosphane chalcogenides: [2-(Et₂NCH₂)C₆H₄]Ph₂PS (**3**), [2-(Et₂NCH₂)C₆H₄]Ph₂PSe (**4**), [2-(Et₂NCH₂)C₆H₄]₂PhPS (**5**) and [2-(Et₂NCH₂)C₆H₄]₂PhPSe (**6**).
- Six new group 11 metal complexes were obtained using the two phosphanes and the appropriate metal salts: [2-(Et₂NCH₂)C₆H₄]Ph₂PCuCl (**7**), [2-(Et₂NCH₂)C₆H₄]Ph₂PAgOTf (**8**), [2-(Et₂NCH₂)C₆H₄]Ph₂PAuCl (**9**), [2-(Et₂NCH₂)C₆H₄]₂PhPCuCl (**10**), [2-(Et₂NCH₂)C₆H₄]₂PhPAgOTf (**11**) and [2-(Et₂NCH₂)C₆H₄]₂PhPAuCl (**12**).
- The NMR studies does not suggest clearly a C,N coordination pattern of the 2-Et₂NCH₂C₆H₄ group in solution, except compound **2**. In the cases of the species with

two 2-Et₂NCH₂C₆H₄ aryl groups, each of them with a pendant arm capable of intramolecular coordination, the NMR spectra suggest their equivalence in solution.

- The solid-state structures of the two triorganophosphane chalcogenides exhibit monomeric structures, with a distorted tetrahedral coordination geometry around phosphorus, with the interatomic distances between phosphorus and sulphur consistent with a double bond.
- The solid-state structures of the two copper complexes present dimeric associations with a distorted tetrahedral environment around each copper atom, while the association takes place through the bridging chlorine atoms. In both compounds the triorganophosphane ligand behaves as a bidentate chelating *P,N* moiety towards the metal centre.
- The X-ray diffraction studies of the gold complex present a molecular structure with a linear geometry about the gold center. In this case the triorganophosphane ligand does not behave as a chelating agent towards the metal center and the molecules are further associated in polymeric chains by CH \cdots Cl interactions.

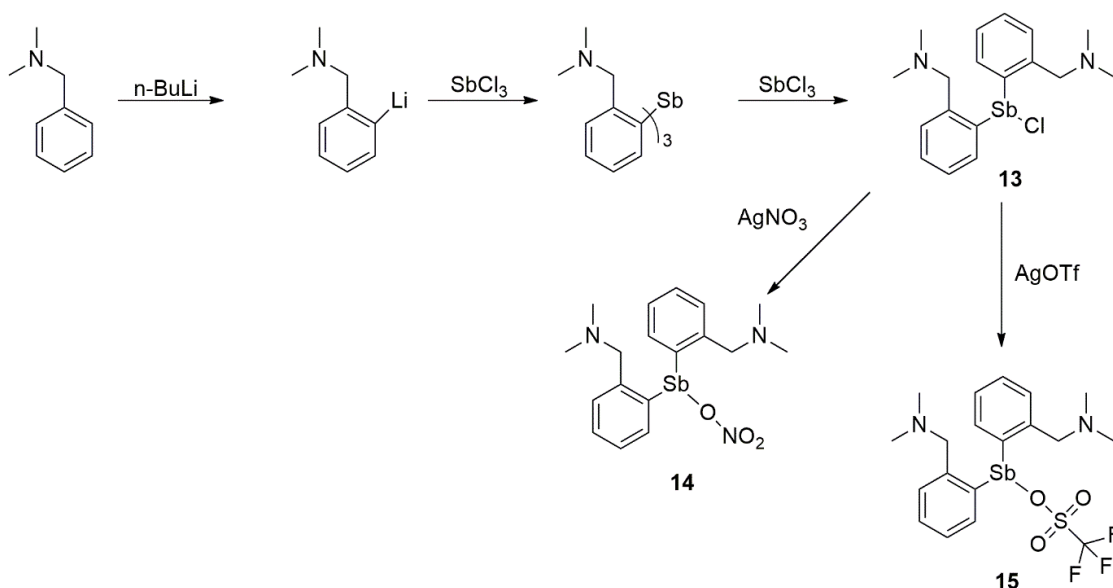
III. Organoantimony compounds

III.2.1. Diorganoantimony compounds with 2-(Me₂NCH₂)C₆H₄ groups

Preparation

The procedures used for the synthesis of the new hypercoordinated antimony(III) compounds, bearing aryl groups with pendant arms with nitrogen donor atoms are depicted in Scheme III.11. The diarylantimony chloride **13** was prepared according to a literature method, starting from [2-(Me₂NCH₂)C₆H₄]₃Sb and SbCl₃.

Compounds **14** and **15** were obtained starting from compound **13** and the appropriate silver salt in a 1:1 molar ratio. All compounds were obtained in good yields, isolated as colorless or white-pink / white-beige solids, well soluble in common organic solvents.



Scheme III.1.

NMR spectroscopy

The solution behavior of compounds **13-15** was investigated by multinuclear NMR spectroscopy (¹H, ¹³C, ¹⁹F where appropriate). The spectra confirmed the presence of the expected compounds. For all three compounds the ¹H NMR exhibit rather broad singlet resonances for the NMe₂ and CH₂ protons, as well as for the aromatic ring proton in position 6, ortho to antimony. This pattern in the NMR spectra at room temperature suggests either a rapid equilibrium between the two nitrogen pendant arms, one coordinated to antimony and the other not, or a rapid dissociation/ re-coordination process of both pendant arms.

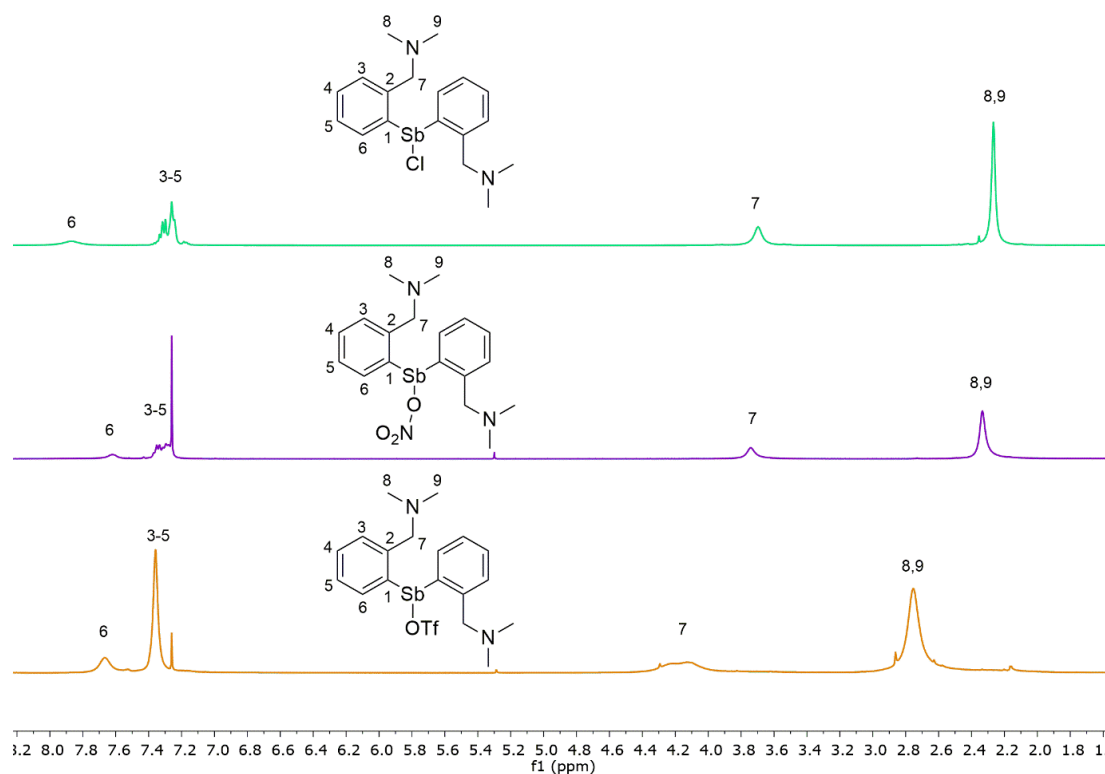


Figure III.1. Stacked ^1H NMR spectra of compounds **13** (top), **14** (middle) and **15** (bottom), in CDCl_3 .

Mass spectrometry

ESI+ MS studies were performed for all three compounds and for each one the spectrum presents the peak characteristic for the expected cation: $[\text{M}-\text{Cl}]^+$ in the case of compound **13**, $[\text{M}-\text{NO}_3]^+$ in case of compound **14**, and $[\text{M}-\text{OTf}]^+$ in case of compound **15**.

IR spectroscopy

The IR spectrum of compound **14** shows strong, broad bands at $1458 / 1285 \text{ cm}^{-1}$, which suggest a chelating bidentate coordination of the anionic NO_3^- ligand.^[74] In the case of compound **15** the IR spectrum also shows strong bands at $1292 / 1030 \text{ cm}^{-1}$, which were assigned to the $\nu_{\text{as}}(\text{SO}_2)$ and $\nu_{\text{s}}(\text{SO}_2)$ vibrations of the triflate anion, thus suggesting a monodentate behavior of this ligand.^[75]

Single-crystal X-ray diffraction studies

The molecular structure of compound **13** was already described previously. In this work, crystals suitable for single-crystal X-ray diffraction studies have been obtained for compounds **14** and the hydrolysis product **15h**. In the case of compound **14**, both nitrogen

atoms of the two 2-(Me₂NCH₂)C₆H₄ substituents are intramolecularly coordinated to the metal centre.

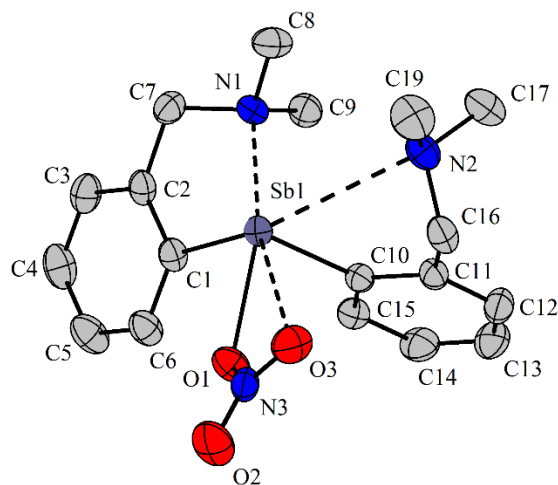


Figure III.2. Ortep-like representation of compound **14**, with thermal ellipsoids at 30% probability level. Hydrogen atoms were omitted for clarity.

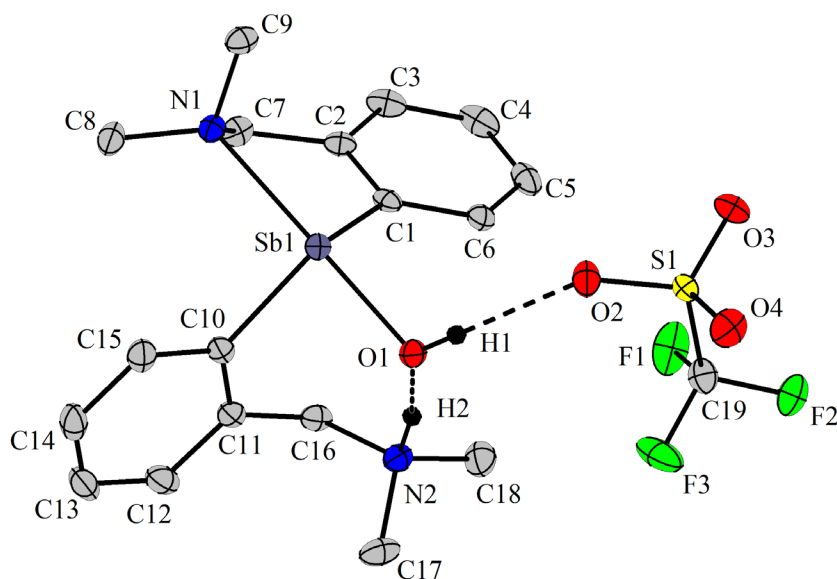


Figure III.3. Ortep-like representation of compound **15h**, with thermal ellipsoids at 50% probability level. Hydrogen atoms were omitted for clarity.

The shorter bond is the one positioned *trans* to the O(1) atom, while the weaker one is the one in *trans* to the C(1) atom. These intramolecular N→Sb interactions give rise to two five-membered NC₃Sb chelate rings which are not planar, but folded along the imaginary Sb⋯C_{methylene} axis, and the nitrogen atom is placed out of the best plane defined by the residual SbC₃ fragment. This induces planar chirality, with the aromatic ring as the chiral plane and the nitrogen atom as the pilot atom. Isomers are given as *S_N*

and R_N .^[47] The other ligand, i.e. the NO_3^- anionic ligand acts as an anisobidentate (chelating) ligand [$\text{O}(1)\text{--Sb}(1)$ 2.375(3) / $\text{O}(3)\text{--Sb}(1)$ 3.145(3) Å, cf. $\Sigma r_{\text{vdw}}(\text{Sb},\text{O})$ 3.60 Å^[12], with the weaker $\text{O}(3)\text{--Sb}(1)$ interaction bisecting the open $\text{N}(2)\cdots\text{Sb}(1)\text{--O}(1)$ bond angle [$120.20(9)^\circ$]. This results in a 14-Sb-6 hypercoordinated species for which the overall coordination geometry can be described as distorted pentagonal pyramidal. The crystal of **14** contains a 1:1 mixture of $(C_{\text{Sb1}})(pS_{\text{N1}},pR_{\text{N2}})\text{-14}$ and $(A_{\text{Sb1}})(pR_{\text{N1}},pS_{\text{N2}})\text{-14}$ isomers.

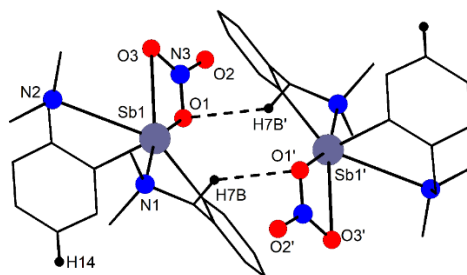


Figure III.4. Dimeric association of $(C_{\text{Sb1}})(pS_{\text{N1}},pR_{\text{N2}})$ and $(A_{\text{Sb1}})(pR_{\text{N1}},pS_{\text{N2}})$ isomers in compound **14** (hydrogen atoms not involved in intermolecular $\text{H}\cdots\text{O}$ contacts were omitted for clarity). Symmetry equivalent positions $-x$, $-y$, $2-z$ are given by “prime”.

Further stabilization of the compound is given by $\pi \text{Sb}\cdots\text{Ph}_{\text{centroid}}$ interactions as well as by intermolecular and intramolecular $\text{H}\cdots\text{O}$ contacts of the two isomers. Further $\text{H}\cdots\text{O}$ inter-dimers contacts of 2.51 Å lead to a supramolecular network (Figure III.5).

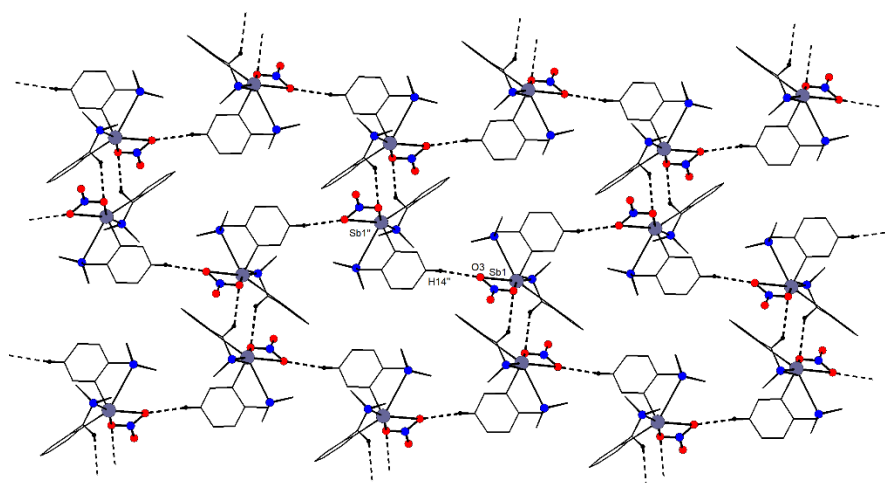


Figure III.5. Best view of a supramolecular layer in the crystal of **14**, built through weak inter-dimers $\text{H}\cdots\text{O}$ contacts of 2.51 Å (only hydrogens involved in hydrogen contacts are shown). Symmetry equivalent positions $-1/2+x$, $1/2-y$, $1/2+z$ are given by “double prime”.

During our attempts to grow single-crystals of compound **15** we obtained a hydrolysis product, the ionic species $[\{2-(\text{Me}_2\text{NH}^+\text{CH}_2)\text{C}_6\text{H}_4\}\{2-(\text{Me}_2\text{NCH}_2)\text{C}_6\text{H}_4\}\text{SbOH}][\text{CF}_3\text{SO}_3]^-$ (**15h**), this was possible through the intermediary formation of the ionic species $[\{2-(\text{Me}_2\text{NCH}_2)\text{C}_6\text{H}_4\}_2\text{Sb}(\text{H}_2\text{O})]^+[\text{CF}_3\text{SO}_3]^-$ followed by the abstraction of one of the hydrogen atoms in the water molecule by the nitrogen in the pendant arm. If we look at the hypercoordinated *10-Sb-4* cation formed, a distorted *pseudo* trigonal bipyramidal (*see-saw*) coordination geometry is formed around the antimony centre, with the hydroxo oxygen and the intramolecularly coordinated nitrogen in apices $[\text{N}(1)\text{--Sb}(1)\text{--O}(1) 159.65(4)^\circ]$. The crystal contains a 1:1 mixture of $(C_{\text{Sb1}})(pS_{\text{N1}})\text{-15h}$ and $(A_{\text{Sb1}})(pR_{\text{N1}})\text{-15h}$ isomers of the cation. Besides the strong hydrogen bond based on the proton at nitrogen in the pendant arm and the oxygen bonded to the metal centre $[\text{H}(2)\cdots\text{O}(1) 1.604 \text{ \AA}, \text{N}(2)\text{--H}(2)\cdots\text{O}(1) 168.00^\circ]$, other weaker hydrogen-oxygen contacts are established between oxygen atoms in the triflate anion and hydrogen atoms in the cations $[\text{O}(2)\cdots\text{H}(1) 2.14 \text{ \AA}, \text{O}3\cdots\text{H}9\text{C} 2.56 \text{ \AA}, \text{O}4\cdots\text{H}17\text{A} 2.55 \text{ \AA}, \text{O}4\cdots\text{H}17\text{C} 2.48 \text{ \AA}]$. Other important interactions can be observed at the supramolecular level, where $\text{C}\text{--H}\cdots\pi$ ($\text{Ar}_{\text{centroid}}$) $[\text{C}(7)\text{--H}(7\text{B})_{\text{methylene}}\cdots\text{Ar}_{\text{centroid}}\{\text{C}(1)\text{--C}(6)\} 2.87 \text{ \AA}, \gamma = 23^\circ]$ contribute to the formation of a supramolecular architecture, in which parallel polymeric chains are connected in a layered, waved structure (Figure III.6 and Figure III.7).

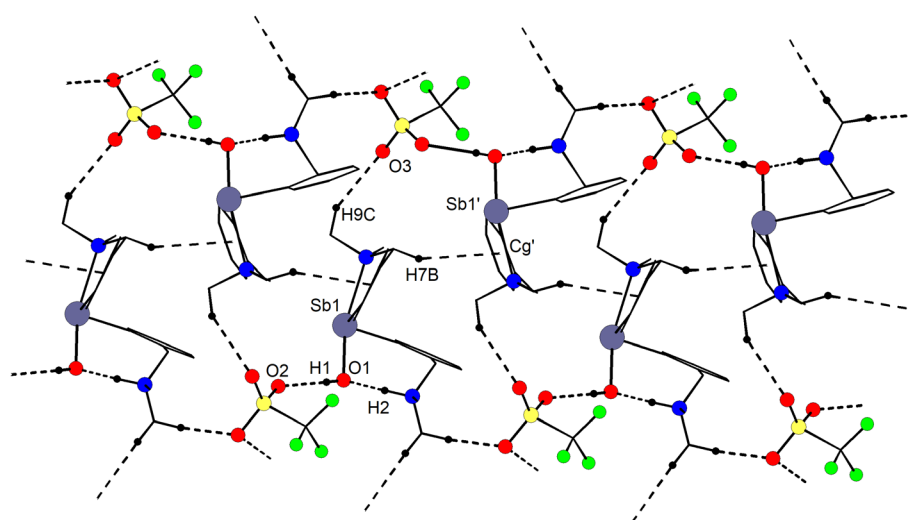


Figure III.6. A layer of the supramolecular network in the crystal of **15h** (view along axis *b*).

Only hydrogens involved in short cation-anion contacts are shown. Symmetry equivalent positions $1/2+x$, $1/2-y$, $1-z$ are given by “prime”.

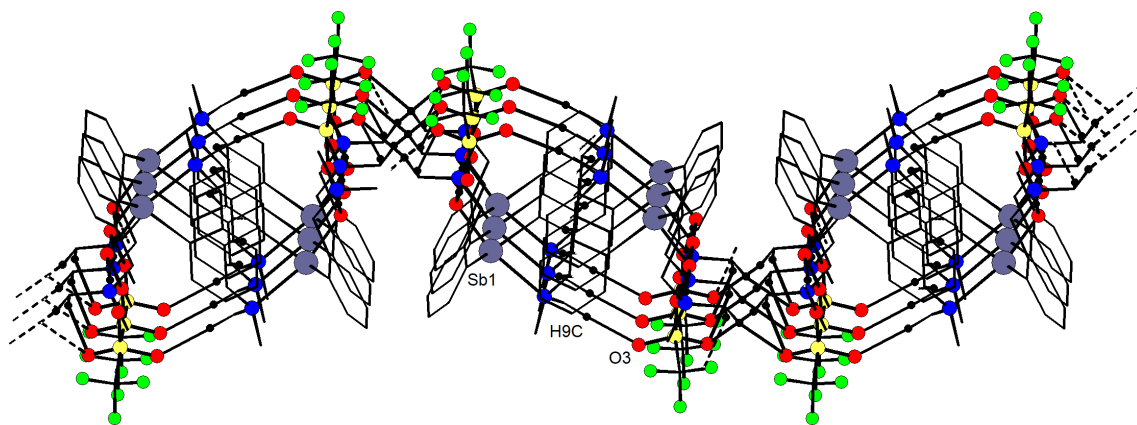
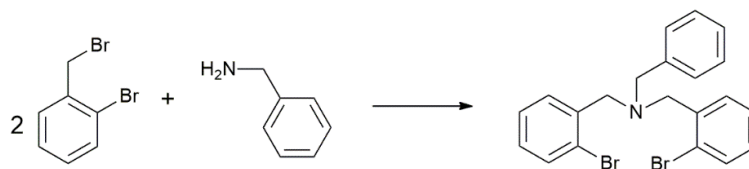


Figure III.7. View along axis *a* of the supramolecular structure of **15h**.

III.2.2. Diorganoantimony compounds containing the $C_6H_5CH_2N(CH_2C_6H_4)_2$ fragment

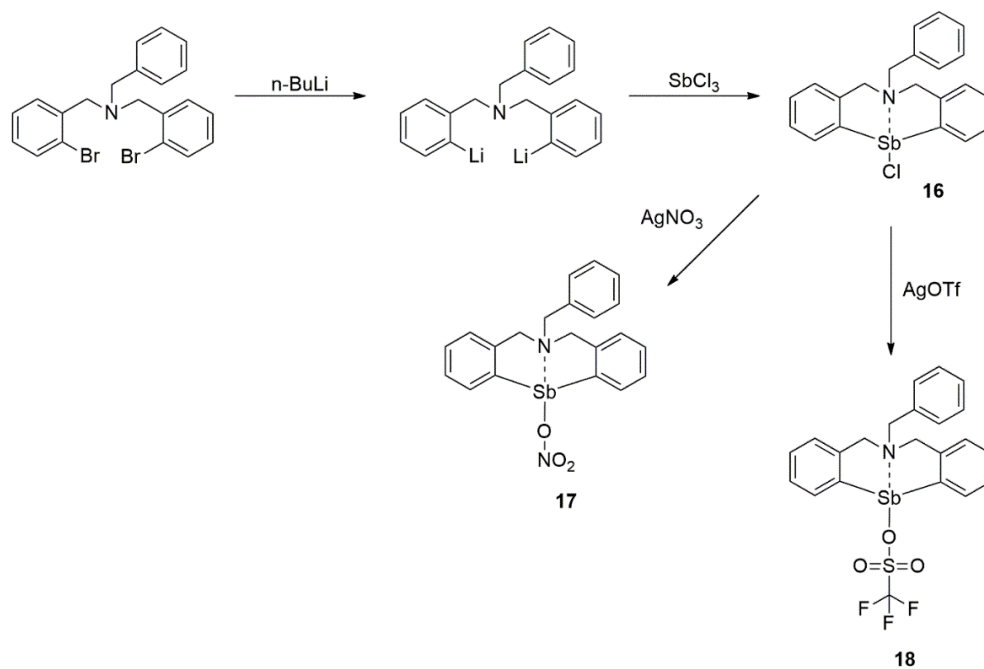
Preparation

The starting organic ligand was synthesized in high yields using a known procedure, i.e. an amine alkylation reaction between 2-bromobenzyl bromide and benzylamine, as depicted in Scheme III.2.^[77]



Scheme III.2.

The new diorganoantimony compounds containing organic groups with nitrogen as a donor atom were prepared according to the following steps: starting from the previously synthesized ligand, the first step required the lithiation of the bromide using *n*-BuLi in the appropriate molar ratio, followed by a second step based on the addition of freshly sublimed $SbCl_3$, thus resulting in the formation of the diorganoantimony chloride **16**. Using the chloride **5** and the appropriate silver salts, compounds **17** and **18** were obtained in very good yields, according to Scheme III.3.



Scheme III.3.

NMR spectroscopy

The ^1H NMR spectra of compounds **16** - **18** (Figure III.8) display an AB spin system for the benzylic protons (H_7), due to the constraints imposed by the formed eight membered ring.

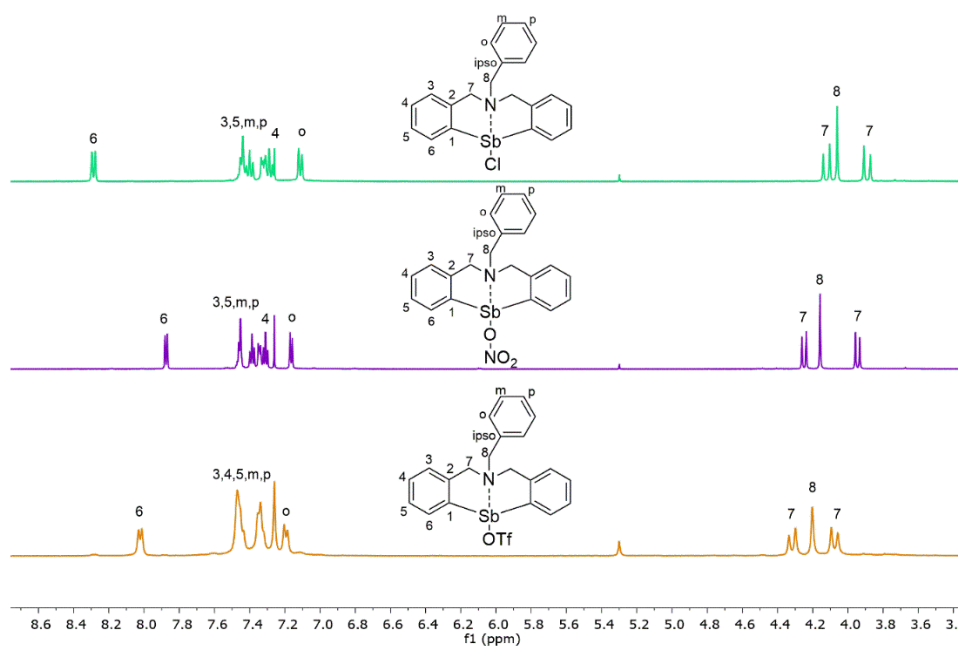


Figure III.8. ^1H NMR spectra of compounds **16** (up), **17** (middle) and **18** (down), in CDCl_3 .

Depending on the inorganic ligand, the signals tend to be more deshielded as we go from Cl^- to OTf^- and further to NO_3^- , and this behavior can be explained by the influence of the intramolecular $\text{N} \rightarrow \text{Sb}$ interaction, which is strongest in compound **16**, then compound **18** and lastly compound **17**, in accordance with the growing electronegative character of the inorganic ligands. The CH_2 protons, H_8 of the pendant arm appear as singlets inside the AB spin system for the benzylic protons H_7 . In the aromatic region, only two sets of resonances are present, indicating that the two phenyl rings attached to antimony are equivalent.

The ^{19}F NMR of compound **18** displays one sharp singlet around -77 ppm, this confirms the presence of fluorine in the compound and the fact that there are no unreacted starting materials with fluorine.

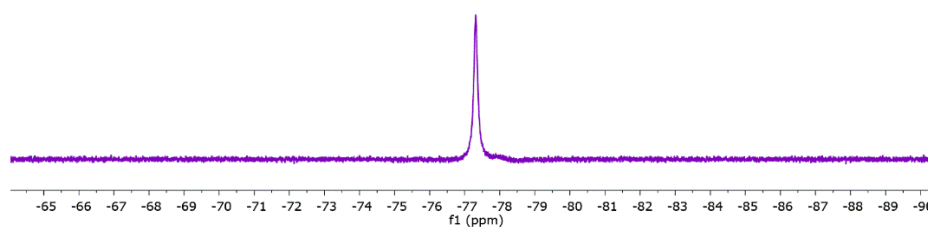


Figure III.9. ^{19}F NMR spectrum of compound **18**, in CDCl_3 .

Mass spectrometry

ESI+ MS studies were performed for all three compounds. In every case the spectrum presents the peaks characteristic for the cation: $[\text{M}-\text{Cl}]^+$ in the case of compound **16**, $[\text{M}-\text{NO}_3]^+$ in the case of compound **17** and $[\text{M}-\text{OTf}]^+$ in the case of compound **18**. One example is presented in Figure III.10.

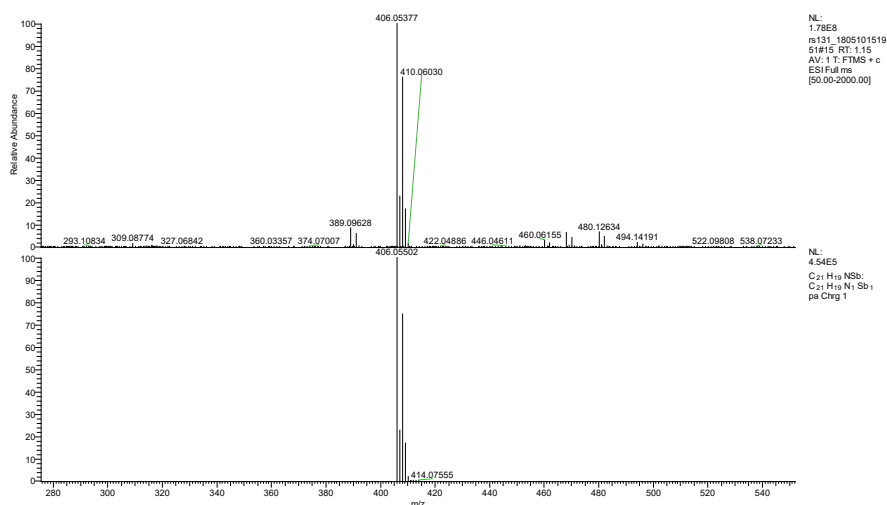


Figure III.10. ESI+ mass spectrum of compound **16** showing the peak at m/z 406.0537 (100) $[\text{M}-\text{Cl}]^+$.

IR spectroscopy

In the IR spectrum compound **17** shows strong, broad bands at 1495 / 1270 cm^{-1} , which might suggest a chelating bidentate coordination of the anionic NO_3^- ligand.^[74] The IR spectrum of compound **18** shows strong bands at 1265 / 1030 cm^{-1} , which were assigned to the $\nu_{\text{as}}(\text{SO}_2)$ and $\nu_{\text{s}}(\text{SO}_2)$ vibrations of the triflate anion.^[75]

Single-crystal X-ray diffraction studies

Suitable crystals for single-crystal X-ray diffraction have been obtained for compounds **16** and **18**. The crystal of compound **16** contains two independent molecules in the unit cell, and they have almost identical molecular parameters, therefore we will discuss the data of one molecule since the two molecules have similar characteristics.

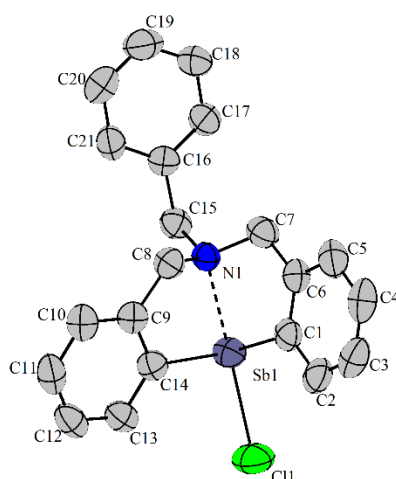


Figure III.11. Ortep-like representation of compound **16** (molecule **16a**), with thermal ellipsoids at 30% probability level. Hydrogen atoms were omitted for clarity.

These compounds display a butterfly-like structure, containing two fused NC_3Sb five-membered rings and, as a consequence, this fact lead to a 10-Sb-4 hypercoordinated species for compound **16**, with a distorted *pseudo* trigonal bipyramidal (*see-saw*) environment about antimony [$\text{Cl}(1)\text{-Sb}(1)\text{-N}(1)$ $160.31(10)^\circ$ in molecule **16a**]. Another important aspect in this molecule is the chirality induced by the nonplanar NC_3Sb five-membered rings, which results in 1:1 racemic mixtures of (pR^1, pR^2) and (pS^1, pS^2) isomers (superscript indices “1” and “2” are assigned for the two fused NC_3Sb rings in a butterfly-like molecule) in the crystal of **16**.

The molecular structure of compound **18** (Figure III.12), shows several similarities with compound **16** with regard to the diorganoantimony(III) fragment.

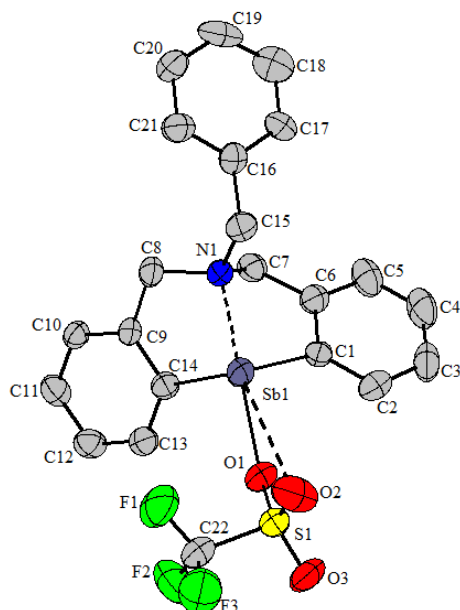


Figure III.12. Ortep-like representation of compound **18**, with thermal ellipsoids at 30% probability level. Hydrogen atoms were omitted for clarity.

The butterfly-like structure is present here as well, containing two fused NC_3Sb five-membered rings. The species can be classified as a *10-Sb-4* hypercoordinated species, with a distorted *pseudo* trigonal bipyramidal (*see-saw*) environment around antimony O(1)–Sb(1)–N(1) $153.5(2)^\circ$ or, due to the presence of the weak Sb(1)⋯O(2) contact ($3.473(6)$ Å, cf. $\Sigma r_{\text{vdW}}(\text{Sb},\text{O})$ 3.60 Å) determined by a bidentate coordination of the OTf ligand, a *12-Sb-5* hypercoordinated species can be assumed. The chirality induced by the nonplanar NC_3Sb five-membered rings results in a 1:1 racemic mixture of (pR^1, pR^2) and (pS^1, pS^2) isomers, as previously described for compound **16**.

For both compounds, supramolecular associations are formed in their crystals.

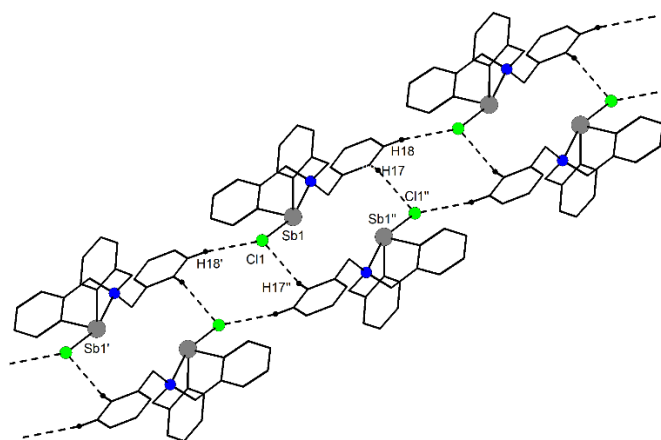
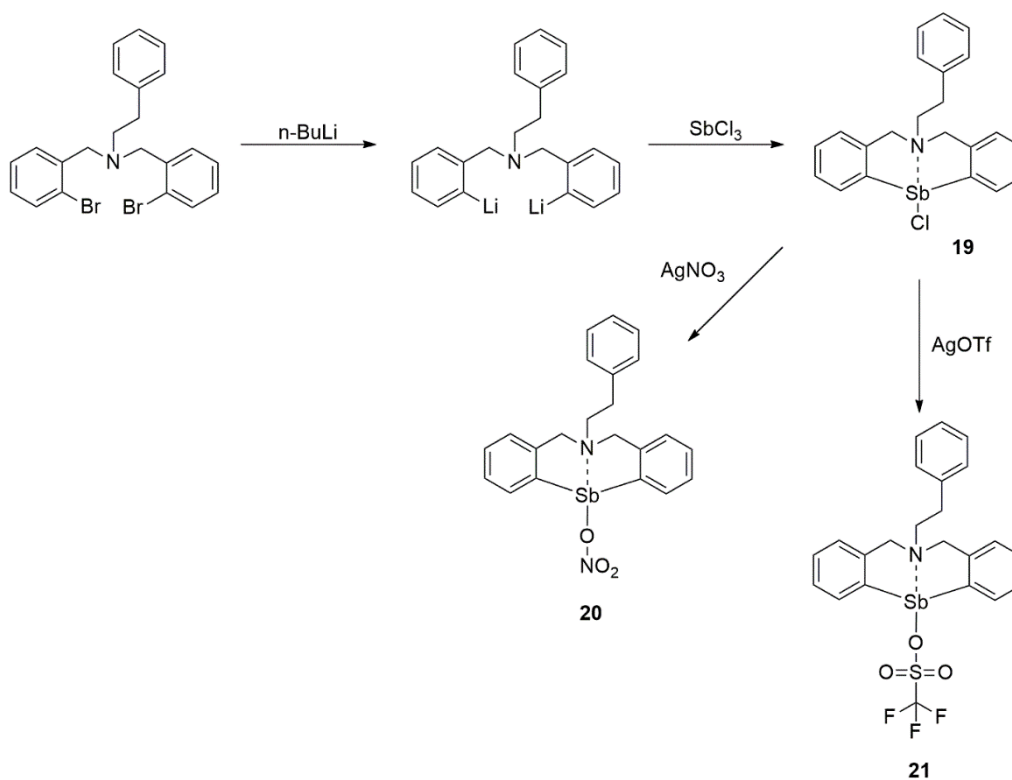


Figure III.13. Ledder-like polymeric association in **16**. Symmetry equivalent positions $x, 1+y, z$; and $2-x, 1-y, 1-z$ are given by “prime” and “double prime”, respectively.

III.2.3. Diorganoantimony compounds containing the $C_6H_5CH_2CH_2N(CH_2C_6H_4)_2$ fragment

Preparation

The starting organic ligand was synthesized from an amine alkylation reaction between 2-bromobenzyl bromide and 2-phenylethylamine. The new diorganoantimony compounds containing organic groups with nitrogen as a donor atom were prepared by the lithiation of the bromide using *n*-BuLi, followed by the addition of freshly sublimed $SbCl_3$, thus resulting in the formation of compound **19**. Reactions between the chloride **19** and the appropriate silver salts were performed as described in Scheme III.4, for the synthesis of compounds **20** and **21**, which were isolated in very good yields.



Scheme III.4.

NMR spectroscopy

The solution behavior of all three new organoantimony compounds was investigated by multinuclear NMR (1H , ^{13}C) spectroscopy. The 1H NMR spectra of compounds **19-21** are shown in Figure III.14.

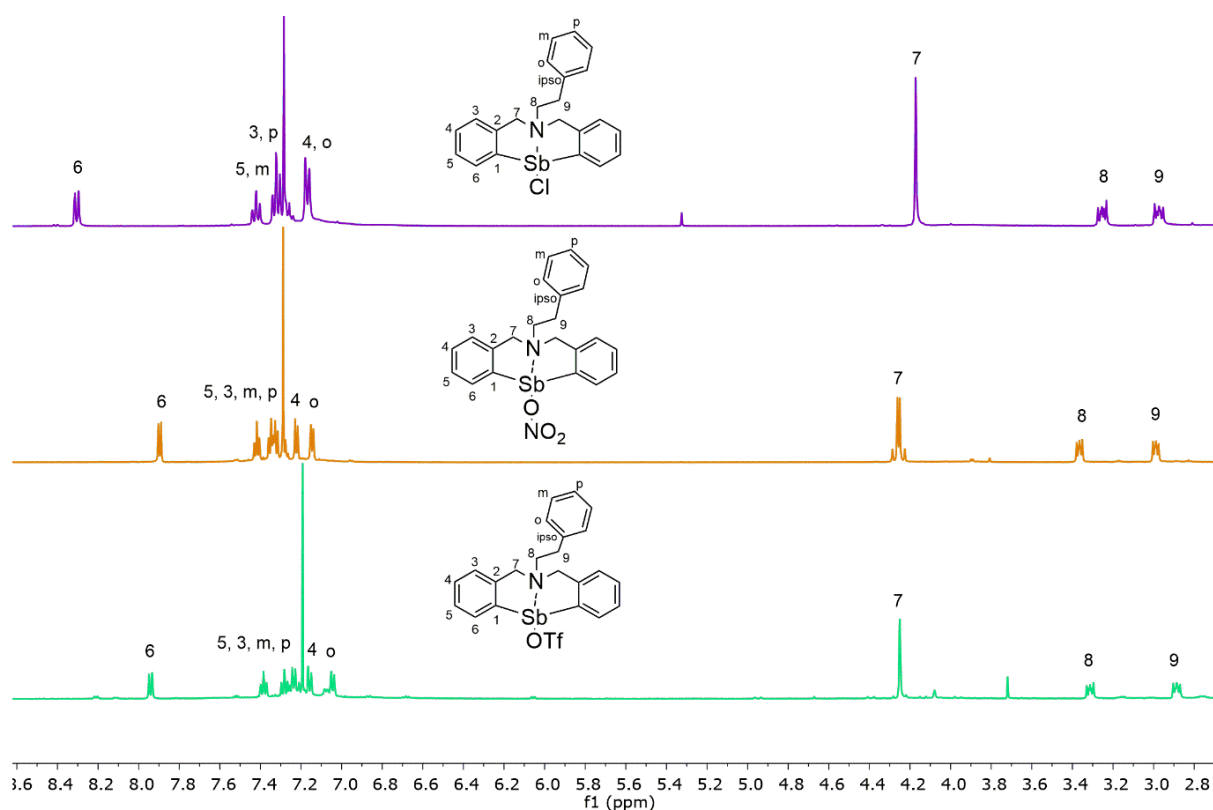


Figure III.14. ^1H NMR spectra of compounds **19** (up), **20** (middle) and **21** (down), in CDCl_3 .

Mass spectrometry

ESI+ MS studies were performed for all three compounds. In every case the spectrum presents the peaks characteristic for the cation: $[\text{M} - \text{Cl}]^+$ in the case of compound **19**, $[\text{M} - \text{NO}_3]^+$ in the case of compound **20**, and $[\text{M} - \text{OTf}]^+$ in the case of compound **21**.

Single-crystal X-ray diffraction studies

Single-crystals were obtained for compound **19**, the diorganoantimony(III) fragment shows similar parameters to other compounds that contain similar fragments, already described in literature, with a strong transannular $\text{N} \rightarrow \text{Sb}$ intramolecular interaction as previously observed in the related species $[\text{RN}(\text{CH}_2\text{C}_6\text{H}_4)_2]\text{SbL}$ ($\text{L} = \text{Cl}$, $\text{R} = \text{'Bu}$, Cy ; $\text{L} = \text{OSO}_2\text{CF}_3$, $\text{R} = \text{Cy}$, Ph).^[63,78] The molecular structure of compound **19** is given in Figure III.15.

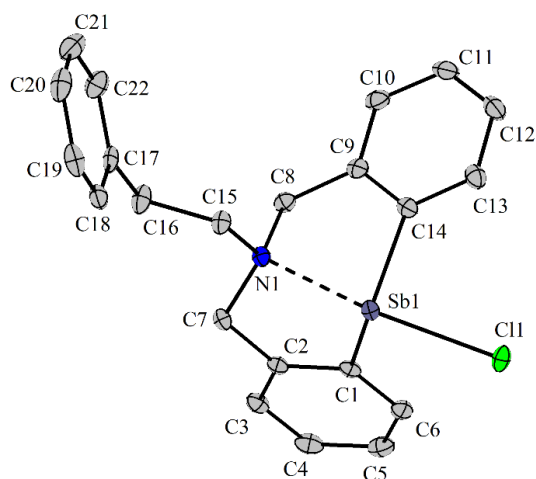
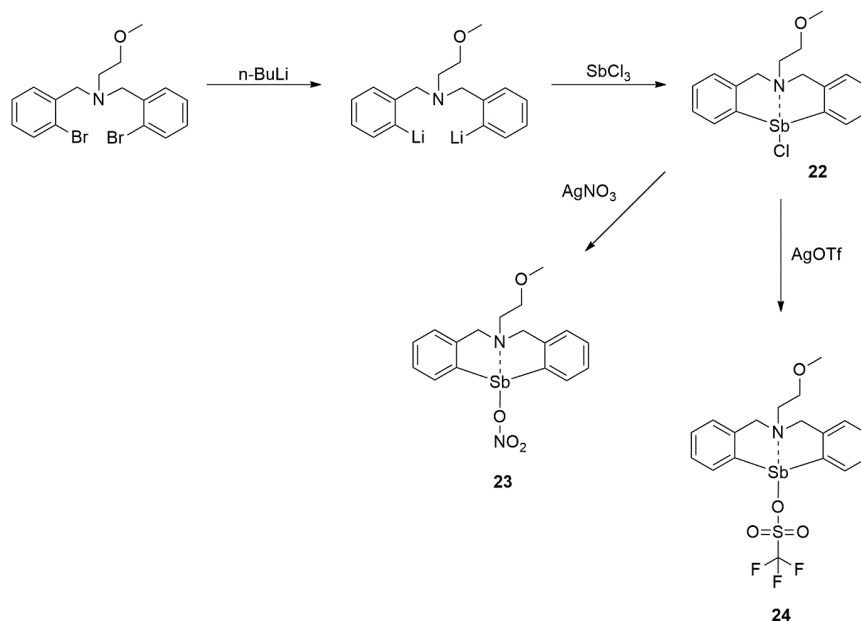


Figure III.15. Ortep-like representation of compound **19**, with thermal ellipsoids at 30% probability level. Hydrogen atoms were omitted for clarity.

III.2.4. Diorganoantimony compounds containing the $\text{CH}_3\text{OCH}_2\text{CH}_2\text{N}(\text{CH}_2\text{C}_6\text{H}_4)_2$ fragment

Preparation

The diorganoantimony compounds were prepared according to a two steps procedure. The first step consisted in the lithiation of the bromide with *n*-BuLi in the appropriate molar ratio, followed by a second step when freshly sublimated SbCl_3 was added, thus resulting the diorganoantimony(III) chloride **22**. Compounds **23** and **24** were obtained in very good yields by reacting compound **22** with the appropriate silver salts, as illustrated in Scheme III.5.



Scheme III.5.

NMR spectroscopy

The solution behavior of all three new organoantimony compounds was investigated by ^1H and ^{13}C NMR spectroscopy as well. The ^1H NMR spectra of compounds **22** - **24** are shown in Figure III.16.

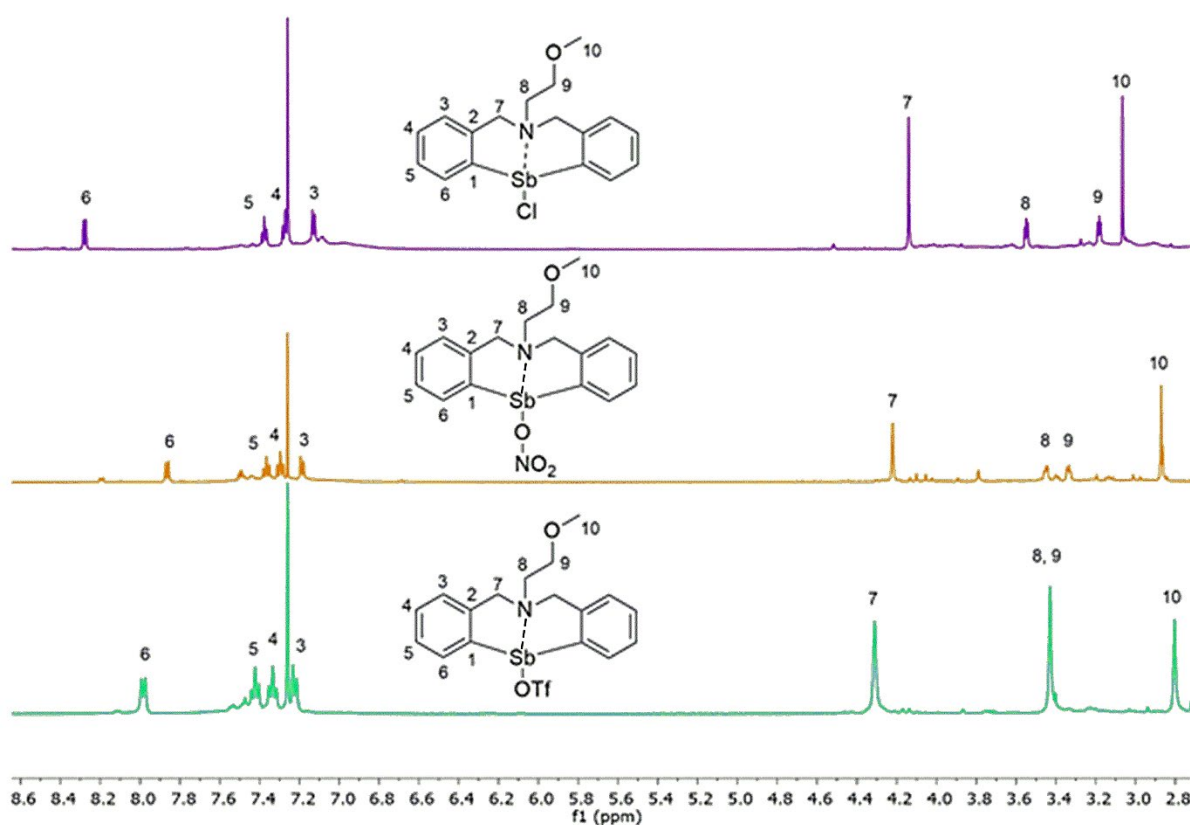


Figure III.16. ^1H NMR spectra of compounds **22** (up), **23** (middle) and **24** (down), in CDCl_3 .

The ^1H NMR spectra of compounds **22** - **24** display the same pattern of signals in all three cases. In the case of compounds **22** and **23**, two multiplet resonances are present, which were attributed to H_9 and H_8 , with the help of 2D NMR. The other two singlet signals were attributed to H_{10} and H_7 . Similarly, to the previously discussed compounds, depending on the inorganic ligand, the signals tend to be more deshielded as we go from Cl^- to OTf^- and further to NO_3^- and such a behaviour can be explained by the influence of the anionic ligand attached to antimony upon the strength of the transannular $\text{N} \rightarrow \text{Sb}$ interaction, which varies in the order **22** > **24** > **23** and is correlated with the variation of the electronegative character of the inorganic ligands.

The ^{19}F NMR spectrum of compound **24** displays one sharp singlet around -77 ppm, slightly shifted when compared with the starting AgOTf . (Figure III.17.)

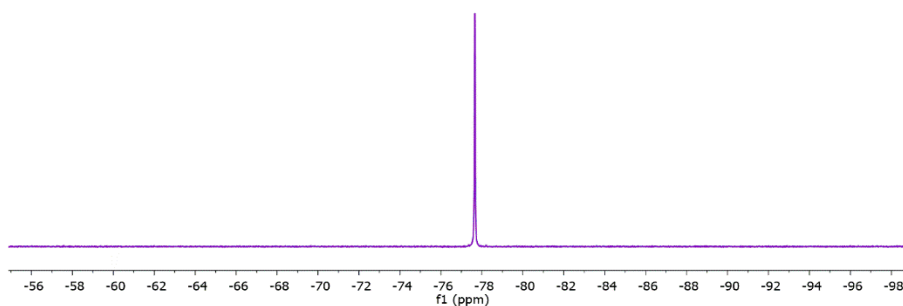


Figure III.17. ^{19}F NMR spectrum of compound **24**, in CDCl_3 .

Mass spectrometry

ESI+ MS studies were performed for all three compounds. In every case the spectra present the peaks characteristic for the cation: $[\text{M} - \text{Cl}]^+$ in the case of compound **22**, $[\text{M} - \text{NO}_3]^+$ in the case of compound **23** and $[\text{M} - \text{OTf}]^+$ in the case of compound **24**.

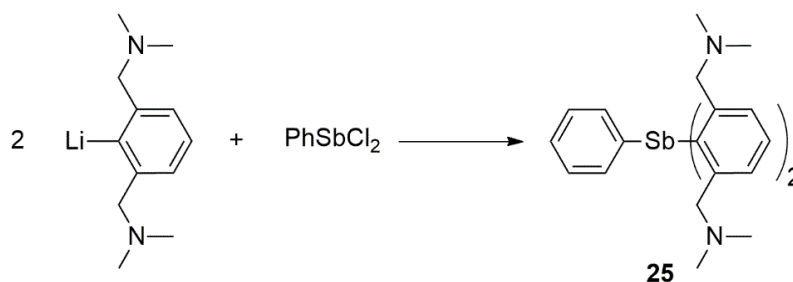
IR spectroscopy

In the IR spectrum compound **23** shows strong, broad bands at $1441 / 1271 \text{ cm}^{-1}$, which might suggest a chelating bidentate coordination of the anionic NO_3^- ligand.^[74] The IR spectrum of compound **24** shows three strong bands at $1288 / 1166 / 1019 \text{ cm}^{-1}$, which were assigned to the $\nu_{\text{as}}(\text{SO}_2)$, $\nu_{\text{s}}(\text{SO}_2)$ and $\nu(\text{SO})$ vibrations of the triflate anion.^[75]

III.2.5. Hypercoordinated triorganoantimony(III) compounds with organic groups bearing two pendant arms

Preparation

The triorganoantimony(III) compound **25** was synthesized by a salt elimination reaction between the organolithium reagent and PhSbCl_2 in 2:1 molar ratio (Scheme III.6). The crude reaction product was mixed with CH_2Cl_2 , thus it was extracted and after removal of the solvent a beige powder was isolated.



Scheme III.6.

NMR spectroscopy

As it can be seen in Figure III.18, in the aliphatic region are present the expected resonances, namely a singlet resonance for the methyl protons H₈ and H₉ in the four equivalent CH₃ groups attached to nitrogen, while the resonance for the CH₂N protons appears as an AB spin system.

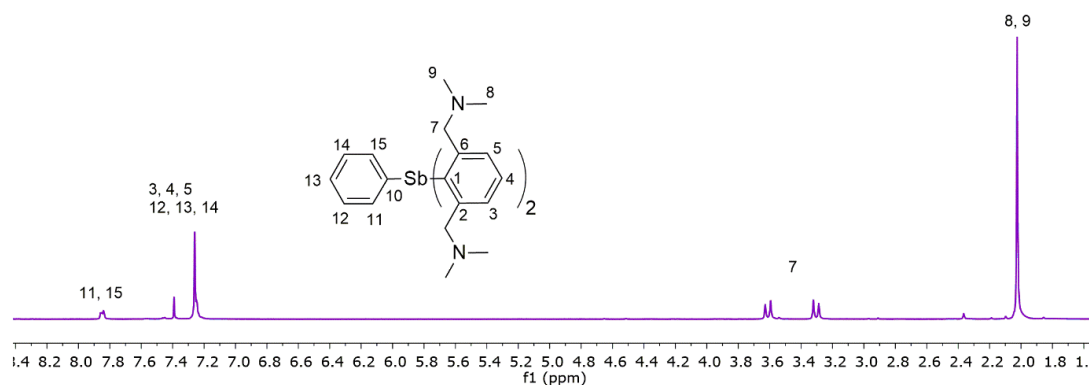


Figure III.18. ¹H NMR spectrum of compound **25**, in CDCl₃.

Mass spectrometry

ESI⁺ MS studies were performed for compound **25**. The spectrum presents the peak characteristic for the ion [M - {(Me₂NCH₂)₂C₆H₃}]⁺ at a m/z value of 389.3333 (100%).

Single-crystal X-ray diffraction studies

Suitable crystals for single-crystal X-ray diffraction were obtained for compound **25**. The two 2,6-(Me₂NCH₂)₂C₆H₃ groups have a different coordination behavior towards the antimony atom; one of them has a *N,C,N* tridentate coordination pattern, while the other is only in a bidentate *C,N* coordination mood attached to the metal. In this way a distorted octahedral geometry is realized about antimony, with three N→Sb interactions, one of the four pendant arms being pushed far away from the coordination sphere of antimony, at a non-bonding distance of 5.02 Å, which is much greater than the sum of the van der Waals radii of the two elements ($\Sigma r_{vdW}(N,Sb) = 3.74 \text{ \AA}$).^[12] Based on the coordination sphere about antimony, this compound can be described as a *14-Sb-6* hypercoordinated species.

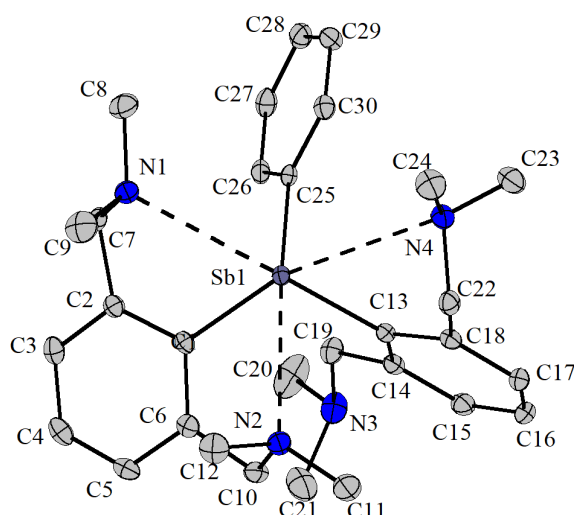
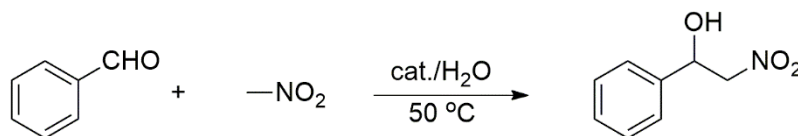


Figure III.19. Ortep-like representation of compound **25**, with thermal ellipsoids at 30% probability level. Hydrogen atoms were omitted for clarity.

III.3. Catalytic results and theoretical calculations

We employed five of the new hypercoordinated diorganoantimony(III) compounds as catalysts in the Henry (nitroaldol) reaction, as displayed in Scheme III.7.



Scheme III.7.

By using a catalytical system that does not use any additional organic solvents we ensure the viability of this process not only from a financial standpoint, but an ecological one as well. The nitroaldol reaction is basically used in organic chemistry as a means of C–C bond formation by the coupling of a nucleophile generated from a nitroalkane with a carbonyl electrophile in base catalysis, thus resulting in β -nitroalcohols which are valuable intermediates in organic synthesis. LDA, TMEDA, alkali metal hydroxides, alkoxides, tetrabutylammonium hydroxide or transition metal complexes were already reported as catalysts in various asymmetric Henry reactions.^[80] Until now no organoantimony compound was employed as a catalyst in the Henry reactions. Five of the new hypercoordinated organoantimony(III) compounds with N→Sb intramolecular interactions described in this work were employed as catalysts in such a transformation, namely [2-(Me₂NCH₂)C₆H₄]₂SbL [L = ONO₂ (**14**), OSO₂CF₃ (**15**)] and [PhCH₂N(CH₂C₆H₄)₂]₂SbL [L = Cl (**16**), ONO₂ (**17**), OSO₂CF₃ (**18**)], which, based on their stability and their dual Lewis acid/base properties, proved to be excellent catalysts.

Our experiments were based on the reaction between benzaldehyde and nitromethane and the products were analysed by GC-MS and NMR spectroscopy. In Table III.1 are given the catalytic results for the Henry addition of nitromethane to benzaldehyde over hypercoordinated organoantimony(III) compounds.

Theoretical calculations of the total atomic charge on antimony and on the weakest coordinated nitrogen, respectively were also performed and the data are displayed in Table III.1. Complexes **13-15** and **16-18**, that have a more positive charged antimony coupled with a more negative charged nitrogen had a direct influence on the increase of the activity (catalysts **14**, **15** and **18**) providing a complete conversion of the benzaldehyde.

The other three catalysts, that have a less positive charge on the antimony centre (catalysts **1**, **5** and **6**) favour dehydration of 1-hydroxy-2-nitro-ethylbenzene to 2-nitrostyrene. Thus, the conclusion that the positive effect of the anion decreases in the following order $\text{OSO}_2\text{CF}_3 > \text{ONO}_2 > \text{Cl}$, catalyst **3** being the one with the highest activity with an excellent TON (turnover number) of around 1.5×10^6 .

Table III.1. Catalytic results for the Henry addition and the theoretical calculations.

Catalysts	Positive charge on Sb / negative charge on N	Conversion of benzaldehyde (%)	Selectivity (%)	
			Nitroaldol	Nitroalkene
13 (water soluble)	0.835 / -0.208	91.3	70.2	29.8
14 (water soluble)	0.939 / -0.211	100	100	0
15 (water soluble)	0.949 / -0.231	100	100	0
16 (no solubility in water)	0.819 / -0.229	89.3	66.8	33.2
17 (no solubility in water)	0.911 / -0.222	94.8	71.8	28.2
18 (no solubility in water)	0.932 / -0.215	100	84.5	15.5
[2-(Me ₂ NCH ₂)C ₆ H ₄]SbCl ₂ (no solubility in water)		0	0	0
Ph ₃ Sb (no solubility in water)		0	0	0
Me ₂ NCH ₂ C ₆ H ₅ (water soluble)		29.7	6.5	93.5
PhCH ₂ N(CH ₂ C ₆ H ₄ Br-2) ₂ (water soluble)		0	0	0

III.4. Conclusions

- Two new hypercoordinated diorganoantimony(III) compounds, namely [2-(Me₂NCH₂)C₆H₄]₂SbL [L = ONO₂ (**14**) and OSO₂CF₃ (**15**)], bearing two aromatic groups with pendant arms capable of N→Sb intramolecular interactions, were prepared, structurally characterized and investigated as catalysts in the Henry reaction.
- Three new hypercoordinated diorganoantimony(III) compounds, namely [C₆H₅CH₂N(CH₂C₆H₄)₂]₂SbL [L = Cl (**16**), ONO₂ (**17**) and OSO₂CF₃ (**18**)], based on a butterfly-like tetrahydro-dibenzo[*c,f*][1,5]-azastibocine heterocyclic framework with a N→Sb transannular interaction were prepared, structurally characterized and investigated as catalysts in the Henry (nitroaldol) reaction.
- Three new hypercoordinated diorganoantimony(III) compounds, namely [C₆H₅CH₂CH₂N(CH₂C₆H₄)₂]₂SbL [L = Cl (**19**), ONO₂ (**20**) and OSO₂CF₃ (**21**)], based on a butterfly-like tetrahydro-dibenzo[*c,f*][1,5]-azastibocine heterocyclic framework with a N→Sb transannular interaction were prepared and structurally characterized.
- Three new hypercoordinated diorganoantimony(III) compounds, namely [CH₃OCH₂CH₂N(CH₂C₆H₄)₂]₂SbL [L = Cl (**22**), ONO₂ (**23**) and OSO₂CF₃ (**24**)], based on a butterfly-like tetrahydro-dibenzo[*c,f*][1,5]-azastibocine heterocyclic framework with a N→Sb transannular interaction were prepared and structurally characterized.
- One new hypercoordinated triorganoantimony(III) compound, namely [2,6-(Me₂NCH₂)₂C₆H₃]₂(Ph)Sb (**25**), with organic groups bearing two pendant arms capable of N→Sb intramolecular interactions, was prepared and structurally characterized.
- The NMR spectra of the compounds are consistent with the proposed species.
- The single-crystal X-ray diffraction studies evidenced two N→Sb intramolecular interactions of different strengths (2.393(3)/ 3.219 Å) in **14**, and only a strong one (2.5454(12) Å) in the hydrolysis product **15h**, in which the nitrogen atom in the second pendant arm is pushed far away from the coordination sphere of antimony.
- The single-crystal X-ray diffraction studies also evidenced strong transannular N→Sb interactions in compounds **16** and **18**.
- The NO₃⁻ ligand in **14** and the CF₃SO₃⁻ ligand in **18** act as bidentate moieties, thus resulting in hexa- and penta-coordinated antimony, while in **15h** and **16** antimony is tetracoordinated by the donor atoms.

- The single-crystal X-ray diffraction studies revealed the formation of *10-Sb-4* hypercoordinated species in **15h**, **16** and **19**, *12-Sb-5* in **18** and *14-Sb-6* in **14** and **25**, respectively.
- Compounds **14-18** were used as catalysts in the Henry reaction and excellent results were obtained, in some cases even with 100% conversion and selectivity.
- The effect of the inorganic ligands, the positive charge on Sb and the negative charge on N were studied and we can conclude that their positive effect on the catalytic process decreases in the following order $\text{OSO}_2\text{CF}_3 > \text{ONO}_2 > \text{Cl}$.
- The strength of the N→Sb transannular interaction depends on the substituents at the antimony atom. In Table III.2 is showed the correlation between the chemical shift of the CH₂ protons (H_{7a}, H_{7b}, H₈ and H₉) and the values of the Hammett constants for the anionic ligands attached to antimony in compounds **16 - 21**. For the crystallographically investigated compounds also the N→Sb distance is given.

Table III.2. Summary of chemical shifts* of CH₂ protons correlated with the Hammett constants.

Compound	Hammett constant, σ_m	H _{7a} $\delta(\text{ppm})$	H _{7b} $\delta(\text{ppm})$	H ₈ $\delta(\text{ppm})$	H ₉ $\delta(\text{ppm})$	$d_{\text{N}\rightarrow\text{Sb}}$ (Å)
R ¹ SbCl (16)	0.37	3.89	4.12	4.06		2.409(4); 2.406(4)
R ¹ SbONO ₂ (17)	0.55	3.93	4.27	4.16		
R ¹ SbOSO ₂ CF ₃ (18)	0.56	4.06	4.33	4.20		2.324(6)
R ² SbCl (19)	0.37	4.17		3.25	2.97	2.398(1)
R ² SbONO ₂ (20)	0.55	4.21	4.25	3.34	2.96	
R ² SbOSO ₂ CF ₃ (21)	0.56	4.29	4.41	3.57	2.94	

R¹ = CH₂C₆H₅; R² = CH₂CH₂C₆H₅; *Spectra were recorded in CDCl₃;

References

1. V. Bhatt, S. Ram, *Chem. Sci. Rev. Lett.*, **2015**, 4(14), 415.
2. R. H. Crabtree, *Organometallic Chemistry of the Transition Metals*, 6th Ed., John Wiley & Sons, New Jersey, Canada, **2014**, Ch. 9, p. 224.
3. A. Bagchi, P. Mukherjee, A. Raha, *Int. J. Recent Adv. Pharm. Res.*, **2015**; 5(3), 171.
4. (a) K.-ya Akiba, *Chemistry of hypervalent compounds*, **1999**, Wiley-VCH, Weinheim.
(b) C. W. Perkins, J. C. Martin, A. J. Arduengo III, W. Lau, A. Alegria, K. Kochi, *J. Am. Chem. Soc.*, **1980**, 102, 7753.
5. (a) S. A. Reiter, B. Assman, S. D. Nogai, N. W. Mitzel, H. Schmidbaur, *Helv. Chim. Acta*, **2002**, 85, 1140.
(b) W. Levason, *Phosphine complexes of transition metals* in F. R. Hartley (Ed.), *The chemistry of organophosphorus compounds*, p. 567, J. Wiley and Sons Ltd., Chichester, **1990**.
6. (a) C. Daniliuc, C. Druckenbrodt, C. G. Hrib, F. Ruthe, A. Blaschette, P. G. Jones, W.-W. du Mont, *Chem. Commun.*, **2007**, 2060.
(b) S. Pohl, W. Saak, R. Lotz, D. Haase, *Z. Naturforsch. B*, **1990**, 45, 1355.
7. (a) C. A. Tolman, *Chem. Rev.*, **1977**, 77, 31.
(b) T.E. Müller, D.M.P. Mingos, *Transition Met. Chem.*, **1995**, 20, 533.
8. Z. Kokan, S. I. Kirin, *Eur. J. Org. Chem.*, **2013**, 8154.
9. (a) C. Chuit, R. J. P. Corriu, P. Monforte, C. Reye, J. P. Declercq, A. Dubourg, *Angew. Chem. Int. Ed. Engl.*, **1993**, 32, 1430.
(b) A. Chandrasekaran, N. V. Timosheva, R. O. Day, R. R. Holmes, *Inorg. Chem.*, **2002**, 41, 5235.
(c) F. Tisato, G. Piloni, F. Refosco, G. Bandoli, C. Corvaja, B. Corain, *Inorg. Chim. Acta*, **1998**, 275-276, 401.
(d) E. Tomas-Mendivil, R. Garcia-Alvarez, S. E. Garcia-Garrido, J. Diez, P. Crochet, V. Cadierno, *J. Organomet. Chem.*, **2013**, 727, 1.
(e) S. Y. de Boer, Y. Gloaguen, M. Lutz, J. I. van der Vlugt, *Inorg. Chim. Acta*, **2012**, 380, 336.

- (f) R. Kreiter, J. J. Firet, M. J. J. Ruts, M. Lutz, A. L. Spek, R. J. M. Klein Gebbink, G. Van Koten, *J. Organomet. Chem.*, **2006**, 691, 422.
- (g) R. Mitea, A. Covaci, C. Silvestru, A. Silvestru, *Rev. Roum. Chim.*, **2013**, 58(2-3), 265.
- (h) L. Horner, G. Simons, *Phosphorus Sulfur Relat. Elem.*, **1983**, 15, 165.
- (i) L. Chen, P. Ai, J. Gu, S. Jie, B.G. Li, *J. Organomet. Chem.*, **2012**, 716, 55.
10. D. W. Allen, Phosphines and related P-C bonded compounds, in D. W. Allen, J. C. Tebby, D. Loakes (Eds.) *Organophosphorus Chemistry*, vol. 40, p. 1-51, RSC Publishing, London, **2011**.
11. F. Carre, C. Chuit, R. J. P. Corriu, A. Mehdi, C. Reye, *J. Organomet. Chem.*, **1997**, 529, 59.
12. J. Emsley, "Die Elemente", Walter de Gruyter, Berlin, **1994**.
13. (a) M. A. Alonso, J. A. Casares, P. Espinet, E. Valles, K. Soulantica, *Tetrahedron Lett.*, **2001**, 42, 5697.
- (b) M. A. Alonso, J. A. Casares, P. Espinet, K. Soulantica, A. G. Orpen, H. Phetmung, *Inorg. Chem.*, **2003**, 42, 3856.
14. L. Brammer, J. C. M. Rivas, C. D. Spilling, *J. Organomet. Chem.*, **2000**, 609, 36.
15. A. F. Ma, H. J. Seo, S. H. Jin, U. C. Yoon, M. H. Hyun, S. K. Kang, Y. I. Kim, *Bull. Korean Chem. Soc.* **2009**, 30, 2754.
16. D. M. Roundhill, R. A. Bechtold, S. G. N. Roundhill, *Inorg. Chem.*, **1980**, 19, 284.
17. (a) G. M. Kapteijn, M. P. R. Spee, D. M. Grove, H. Kooijman, A. L. Spek, G. van Koten, *Organometallics*, **1996**, 15, 1405.
- (b) J. Pfeiffer, G. Kickelbick, U. Schubert, *Organometallics*, **2000**, 19, 62.
18. (a) H. Lang, M. Leschke, H. A. Mayer, M. Melter, C. Weber, G. Rheinwald, O. Walter, G. Huttner, *Inorg. Chim. Acta*, **2001**, 324, 266.
- (b) H. Lang, M. Leschke, G. Rheinwald, M. Melter, *Inorg. Chem. Commun.*, **1998**, 1, 254.
- (c) M. Leschke, M. Melter, B. Walfort, A. Driess, G. Huttner, H. Lang, *Z. Anorg. Allg. Chem.*, **2004**, 630, 2022.
- (d) H. Lang, M. Leschke, M. Melter, B. Walfort, K. Kohler, S. E. Schulz, T. Gessner, *Z. Anorg. Allg. Chem.*, **2003**, 629, 2371.
- (e) M. Leschke, M. Melter, C. Weber, G. Rheinwald, H. Lang, *Z. Anorg. Allg. Chem.*, **2001**, 627, 1199.

- (f) M. Leschke, H. Lang, M. Melter, G. Rheinwald, C. Weber, H. A. Mayer, H. Pritzkow, L. Zsolnai, A. Driess, G. Huttner, *Z. Anorg. Allg. Chem.*, **2002**, 628, 349.
- (g) H. Lang, Y. Shen, T. Ruffer, B. Walfort, *Inorg. Chim. Acta*, **2008**, 361, 95.
- (h) M. Leschke, G. Rheinwald, H. Lang, *Z. Anorg. Allg. Chem.*, **2002**, 628, 2470.
19. A. Dobri, Al. Covaci, A. Covaci, A. Silvestru, *Polyhedron*, **2020**, 182, 114511.
20. A. Covaci, R. Mitea, I. Hosu, A. Silvestru, *Polyhedron*, **2014**, 72, 157.
21. J. McNulty, K. Keskar, *Org. Biomol. Chem.*, **2013**, 11, 2404.
22. Y. Jang, P. Kim, Y. Jeong, H. Lee, *J. Mol. Catal. A: Chem.*, **2003**, 206, 29.
23. H. Yang, N. Lugan, R. Mathieu, *Organometallics*, **1997**, 16, 2089.
24. T. Lager, G. Helmchen, *Tetrahedron Lett.*, **1996**, 37, 1381.
25. Y. Nishibayashi, K. Segawa, K. Ohe, S. Uemura, *Organometallics*, **1995**, 14, 5486.
26. J. Andrieu, J.-M. Camus, P. Richard, R. Poli, L. Gonsalvi, F. Vizza, M. Peruzzini, *Eur. J. Inorg. Chem.*, **2006**, 51.
27. M. Iwaoka, S. Tomoda, *J. Am. Chem. Soc.*, **1996**, 118, 8077.
28. G. S. Ananthnag, N. Edukondalu, J.T. Mague, M. S. Balakrishna, *Polyhedron*, **2013**, 62, 203.
29. I. Yamada, M. Ohkouchi, M. Yamaguchi, T. Yamagishi, *J. Chem. Soc., Perkin Trans.*, **1997**, 1, 1869.
30. S. Maggini, *Coord. Chem. Rev.*, **2009**, 253, 1793.
31. L. O. de la Tabla, I. Matas, P. Palma, E. Alvarez, J. Campora, *Organometallics*, **2012**, 31, 1006.
32. L. J. Hounjet, R. McDonald, M. J. Ferguson, M. Cowie, *Inorg. Chem.*, **2011**, 50, 5361.
33. M. A. del Águila-Sánchez, N. M. Santos-Bastos, M. C. Ramalho-Freitas, J. G. López, M. C. de Souza, J.A. L. Camargos-Resende, M. Casimiro, G. Alves-Romeiro, M. J. Iglesias, F. L. Ortiz, *Dalton Trans.*, **2014**, 43, 14079.
34. A.T. Breshears, A.C. Behrle, C.L. Barnes, C.H. Laber, G.A. Baker, J.R. Walensky, *Polyhedron*, **2015**, 100, 333.
35. J. Won, D. Noh, J. Yun, J. Yong Lee, *J. Phys. Chem. A*, **2010**, 114, 12112.
36. J. X. Chen, J. F. Daeuble, J. M. Stryker, *Tetrahedron*, **2000**, 56, 2789.
37. K. Ramakrishna, C. Sivasankar, *J. Organomet. Chem.*, **2016**, 805, 122.
38. D. M. Zink, M. Bächle, T. Baumann, M. Nieger, M. Kühn, C. Wang, W. Klopfer, U. Monkowius, T. Hofbeck, H. Yersin, S. Bräse, *Inorg. Chem.*, **2013**, 52, 2292.
39. F. Wei, X. Liu, Z. Liu, Z. Bian, Y. Zhao, C. Huang, *CrystEngComm.*, **2014**, 16, 5338.

40. K. J. Kilpin, B. P. Jarman, W. Henderson, B. K. Nicholson, *Appl. Organomet. Chem.* **2011**, *25*, 810.
41. A. S. K. Hashmi, *Chem. Rev.*, **2007**, *107*, 3180.
42. M. Rudolph, A. S. K. Hashmi, *Chem. Commun.*, **2011**, *47*, 6536.
43. C. M. Wehman-Ooyevaar, I. F. Luitwieler, K. Vatter, D.M. Grove, W. J. J. Smeets, E. Horn, L. A. Spek, G. van Koten, *Inorg. Chim. Acta*, **1996**, *252*, 55.
44. A. Rotar, A. Covaci, A. Pop, A. Silvestru, *Rev. Roum. Chim.* **2010**, *55*, 823.
45. B. Ziemer, A. Rabis, H. U. Steinberger, *Acta Cryst. C*, **2000**, *56*, e58.
46. A. N. Skvortsov, A. N. Reznikov, D. A. de Vekki, A. I. Stash, V. K. Belsky, V. N. Spevak, N. K. Skvortsov, *Inorganica Chim. Acta*, **2006**, *359*, 1031.
47. IUPAC Nomenclature of Organic Chemistry, *Pergamon Press*, Oxford, **1979**.
48. I. Haiduc, J. J. Zuckerman, *Basic Organometallic Chemistry*, Walter de Gruyter, Berlin, **1985**.
49. C. I. Raț, C. Silvestru, H. J. Breunig, *Coord. Chem. Rev.*, **2013**, *257*, 818.
50. L. Dostal, R. Jambor, A. Ruzicka, M. Erben, R. Jirasko, E. Cernoskova, J. Holecek, *Organometallics*, **2009**, *28*, 2633.
51. J. Beckmann, J. Bolsinger, A. Duthie, *Z. Anorg. Allg. Chem.*, **2010**, *636*, 765.
52. A. E. Ghionoiu, D. L. Popescu, C. Maxim, A. M. Madalan, I. Haiduc, M. Andruh, *Inorg. Chem. Commun.*, **2015**, *58*, 71.
53. H. Matsuda, A. Ninagawa, R. Nomura, *Chem. Lett.*, **1979**, 1261.
54. H. Matsuda, A. Ninagawa, H. Hasegawa, *Bull. Chem. Soc. Jpn.*, **1985**, *58*, 2717.
55. Y. Chen, R. Qiu, X. Xu, C.T. Au, S. F. Yin, *RSC Adv.*, **2014**, *4*, 11907.
56. R. Nomura, S. I. Miyazaki, T. Nakano, H. Matsuda, *Appl. Organomet. Chem.*, **1991**, *5*, 513.
57. R. Nomura, Y. Wada, H. Matsuda, *J. Polym. Sci. A Polym.*, **1988**, *26*, 627.
58. S. Yasuike, Y. Kishi, S. Kawara, J. Kurita, *Chem. Pharm. Bull.*, **2005**, *53(4)*, 425.
59. K. Ohkata, M. Ohnishi, K. Akiba, *Tetrahedron Lett.*, **1988**, *29*, 5401.
60. J. Xia, R. Qiu, S. Yin, X. Zhang, S. Luo, C. T. Au, K. Xia, W. Y. Wong, *J. Organomet. Chem.*, **2010**, *695*, 1487.
61. R. Qiu, Y. Chen, S. F. Yin, X. Xu, C. T. Au, *RSC Adv.*, **2012**, *2*, 10774.
62. (a) K. Ohkata, S. Takemoto, M. Ohnishi, K.-ya Akiba, *Tetrahedron Lett.*, **1981**, *30*, 4841.
- (b) C. Hansch, A. Leo, R. W. Taft, *Chem. Rev.*, **1991**, *91(2)*, 165.
63. N. Tan, T. Nie, C. T. Au, D. Lan, S. Wua, B. Yi, *Tetrahedron Lett.* **2017**, *58*, 2592.

64. M. Matsumura, R. Takada, Y. Ukai, M. Yamada, Y. Murata, N. Kakusawa, S. Yasuike, *Heterocycles*, **2016**, *93*, 1.
65. M. Fujiwara, A. Baba, H. Matsuda, *Bull. Chem. Soc. Jpn.*, **1990**, *63*, 1069.
66. M. Yang, N. Pati, G. Belanger-Chabot, M. Hirai, F. P. Gabbai, *Dalton Trans.*, **2018**, *47*, 11843.
67. C. Leroy, R. Johansson, D. L. Bryce, *J. Phys. Chem. A*, **2019**, *123*, 1030.
68. A. Bauza, T. J. Mooibroek, A. Frontera, *ChemPhysChem*, **2016**, *17*, 1608.
69. M. Yang, D. Tofan, C.-H. Chen, K. M. Jack, F. P. Gabbai, *Angew. Chem., Int. Ed.*, **2018**, *57*, 13868.
70. J. Y. C. Lim, P. D. Beer, *Chem.*, **2018**, *4*, 731.
71. A. Gini, M. Paraja, B. Galmes, C. Besnard, A. I. Poblador-Bahamonde, N. Sakai, A. Frontera, S. Matile, *Chem. Sci.*, **2020**, *11*, 7086.
72. N. Tan, Y. Chen, S. Yin, R. Qiu, Y. Zhou, C. T. Au, *Curr. Org. Chem.*, **2012**, *16*, 2462.
73. L. Opris, A. Silvestru, C. Silvestru, H. Breunig, E. Lork, *Dalton Trans.*, **2003**, 4367.
74. (a) K. Nakamoto, *Infrared and Raman Spectra of Inorganic and Coordination Compounds – Part B*, 6th ed., John Wiley & Sons, Hoboken, NJ, USA, **2009**, 92.
(b) H. J. Breunig, M. G. Nema, C. Silvestru, A. P. Soran and R. A. Varga, *Dalton Trans.*, **2010**, *39*, 11277.
75. (a) P.-A. Bergstrom, J. Lindgren, *J. Mol. Struct.*, **1990**, *239*, 103.
(b) S. P. Gejji, K. Hermansson, J. Lindgren, *J. Phys. Chem.*, **1993**, *97*, 3712.
76. C. J. Carmalt, A. H. Cowley, R. D. Culp, R. A. Jones, S. Kamepalli, N. C. Norman, *Inorg. Chem.*, **1997**, *36*, 2770.
77. F. H. Carré, R. J. P. Corriu, G. F. Lanneau, P. Merle, F. Soulairol, J. Yao, *Organometallics*, **1997**, *16*, 3878.
78. (a) Y. Chen, K. Yu, N.-Y. Tan, R.-H. Qiu, W. Liu, N.-L. Luo, L. Tong, C.-T. Au, Z.-Q Luo, S.-F. Yin, *Eur. J. Med. Chem.*, **2014**, *79*, 391.
(b) N. Kakusawa, S. Yasuike, J. Kurita, *Heterocycles*, **2010**, *80*, 163.
79. (a) N. Kakusawa, Y. Tobiyasu, S. Yasuike, K. Yamaguchi, H. Seki, J. Kurita, *Tetrahedron Lett.*, **2003**, *44*, 8589.
(b) N. Kakusawa, Y. Tobiyasu, S. Yasuike, K. Yamaguchi, H. Seki, J. Kurita, *J. Organomet. Chem.*, **2006**, *691*, 2953.
80. (a) J. Boruwa, N. Gogoi, P. P. Saikia, N. C. Barua, *Tetrahedron: Asymmetry*, **2006**, *17*, 3315.

- (b) A. Majhi, S. T. Kadam, S. S. Kim, *Bull. Korean Chem. Soc.*, **2009**, *30*, 1767.
- (c) P. Sakthipriya, S. Joseph, N. Ananthi, *MOJ Biorg. Org. Chem.*, **2017**, *1(6)*, 218.
81. MestReNova, Mestrelab Research S.L., Feliciano Barrera 9B – Bajo, 15706 Santiago de Compostela, Spain, <https://mestrelab.com>.
82. G. M. Sheldrick, *Acta Crystallogr. Sect. C Struct. Chem.*, **2015**, *71*, 3–8.
83. A. L. Spek, *Acta Crystallogr. Sect. D Biol. Crystallogr.*, **2009**, *65*, 148–155.
84. Diamond - Crystal and Molecular Structure Visualization, Crystal Impact, Kreuzherrenstr. 102, 53227 Bonn, Germany, **2006**.
85. M. J. Frisch, G. W. Trucks, H. B. Schlegel, G. E. Scuseria, M. A. Robb, J. R. Cheeseman, G. Scalmani, V. Barone, B. Mennucci, G. A. Petersson, H. Nakatsuji, M. Caricato, X. Li, H. P. Hratchian, A. F. Izmaylov, J. Bloino, G. Zheng, J. L. Sonnenberg, M. Hada, M. Ehara, K. Toyota, R. Fukuda, J. Hasegawa, M. Ishida, T. Nakajima, Y. Honda, O. Kitao, H. Nakai, T. Vreven, J. A. Montgomery, Jr., J. E. Peralta, F. Ogliaro, M. Bearpark, J. J. Heyd, E. Brothers, K. N. Kudin, V. N. Staroverov, T. Keith, R. Kobayashi, J. Normand, K. Raghavachari, A. Rendell, J. C. Burant, S. S. Iyengar, J. Tomasi, M. Cossi, N. Rega, J. M. Millam, M. Klene, J. E. Knox, J. B. Cross, V. Bakken, C. Adamo, J. Jaramillo, R. Gomperts, R. E. Stratmann, O. Yazyev, A. J. Austin, R. Cammi, C. Pomelli, J. W. Ochterski, R. L. Martin, K. Morokuma, V. G. Zakrzewski, G. A. Voth, P. Salvador, J. J. Dannenberg, S. Dapprich, A. D. Daniels, O. Farkas, J. B. Foresman, J. V. Ortiz, J. Cioslowski and D. J. Fox, *Gaussian 09, Revision E.01*, Gaussian, Inc., Wallingford, CT, **2013**.
86. A. D. Becke, *J. Chem. Phys.*, **1993**, *98*, 5648.
87. F. Weigend, R. Ahlrichs, *Phys. Chem. Chem. Phys.*, **2005**, *7*, 3297.
88. S. Grimme, S. Ehrlich, L. Goerigk, *J. Comput. Chem.*, **2011**, *32*, 1456.

List of relevant publications

1. Triarylphosphanes with 2-(Et₂NCH₂)C₆H₄ groups. Copper(I) complexes and oxidation derivatives of type EP(C₆H₄CH₂NEt₂-2)_nPh_{3-n} (E = S, Se; n = 1,2). **R. Şuteu**, S. Shova, A. Silvestru, *Inorg. Chim. Acta*, **2018**, 475, 105-111. F.I. = 3.118.
2. Hypercoordinated diorganoantimony(III) compounds of types [2-(Me₂NCH₂)C₆H₄]₂SbL and [PhCH₂N(CH₂C₆H₄)₂]₂SbL (L = Cl, ONO₂, OSO₂CF₃). Synthesis, structure and catalytic behaviour in the Henry reaction. **R. Şuteu**, C. I. Raţ, C. Silvestru, A. Simion, N. Candu, V. I. Pârvulescu, A. Silvestru, *Appl. Organomet. Chem.*, **2020**, 34(4), e5393, F.I. = 4.072.
3. Hypercoordinated diorganopnicogen(III) compounds based on a butterfly-like skeleton of type [CH₃OCH₂CH₂N(CH₂C₆H₄)₂]₂M (M = Sb, Bi). **R. Şuteu**, A. M. Toma, M. Mehning, A. Silvestru, *J. Organomet. Chem* **2020**, 920, 121343. F.I. = 2.345.

Note: The Impact Factors are those reported for 2021.

List of relevant conferences

1. The 12th International Symposium of the Romanian Catalysis Society – RomCat 2019, Bucharest, June 2019: Hypercoordinated diorganoantimony(III) compounds as catalysts for the Henry reaction. **Răzvan Şuteu**, Natalia Candu, Vasile Pârvulescu, Anca Silvestru – poster.
2. Young Researchers' International Conference on Chemistry and Chemical Engineering (YRICCCE II), Budapest, May 2018: Hypervalent compounds with N→Sb interactions. **Răzvan Şuteu**. – oral presentation.
3. European Workshop on Phosphorus Chemistry – EWPC 14, Cluj-Napoca, March 2017: Group 12 Metal Complexes with Hypervalent Triarylphosphanes. **Răzvan Şuteu** – poster.
4. Young Researchers' International Conference on Chemistry and Chemical Engineering (YRICCCE I), Cluj-Napoca, May 2016: Hypervalent triarylphosphanes and their group 12 metal complexes. **Răzvan Şuteu**. – oral presentation.